DANMARKS OG GRØNLANDS GEOLOGISKE UNDERSØGELSE RAPPORT 2012/60

Evaluation of the mineral potential in the Bjørnesund Greenstone Belt combining mineral potential mapping, field work and lithogeochemistry

Dennis Martin Schlatter & Bo Møller Steensgaard

GEOLOGICAL SURVEY OF DENMARK AND GREENLAND
DANISH MINISTRY OF CLIMATE, ENERGY AND BUILDING

GEUS

DANMARKS OG GRØNLANDS GEOLOGISKE UNDERSØGELSE RAPPORT 2012/60

Evaluation of the mineral potential in the Bjørnesund Greenstone Belt combining mineral potential mapping, field work and lithogeochemistry

Dennis Martin Schlatter* & Bo Møller Steensgaard

* Denis Martin Schlatter: former GEUS, presently at Helvetica Exploration Services GmbH, Carl-Spitteler-Strasse 100, CH-8053 Zürich, Switzerland.
Email: denis.schlatter@helvetica-exploration.ch

GEOLOGICAL SURVEY OF DENMARK AND GREENLAND
DANISH MINISTRY OF CLIMATE, ENERGY AND BUILDING

GEUS

Content

* Denis Martin Schlatter: former GEUS, presently at Helvetica Exploration Services GmbH, Carl-Spitteler-Strasse 100, CH-8053 Zürich, Switzerland. Email: denis.schlatter@helvetica-exploration.ch

Abstract

The Bjørnesund area is dominated by amphibolites containing bodies and slivers of ultramafic to mafic rocks. Based on regional qualitative and quantitative mineral potential mapping for gold the Bjørnesund West and East areas were selected for field work in 2009 by a two men team from GEUS. The objectives with the field work was to provide new detailed information, sampling and mapping from the area in order to characterise the geological environment, follow up on results from the mineral potential mapping and processed remote sensing data and evaluate the possibilities for gold mineralisations in the areas. A newly compiled, detailed and geo-referenced digital geological map is presented in this report.

New sites with rock samples elevated in gold have been identified from the work. The most interesting gold occurrences were found in a hydrothermally-altered shear zone. This several tens-of-metre wide shear zone is located in the Bjørnesund West area at 50°16.2'W and 62°54.4'N at 555 m elevation above sea level. The shear zone trends northeast-southwest and dips 80 degrees towards the southeast. It can be followed over several hundreds of metres along strike. This shear zone contains a 50 cm yellow-brownish, rusty stained amphibolite, which hosts parallel quartz-carbonate-feldspar veinlets. Chip samples over 50 cm, within the amphibolite hosted quartz-carbonate-feldspar veined shear zone yield 569 ppb Au. Alteration related to this Au-mineralization is of the Grt, Bt, Iron oxide-hydroxide type. Similar amphibolite 1.5 km towards southwest yields 31 ppb over an about 10 m chip sample profile. A sample taken from a meta-ultramafic unit about 1.4 km towards the northeast yields 134 ppb Au. Scree sediment samples within this zone return 71 ppb and 50 ppb gold confirming the potential of this area to host gold. Some of the amphibolite units exhibit extensive rust zoning due to surface weathering, but are barren in gold.

Although the field work reported here focuses on the assessment of the gold potential in the Bjørnesund area, it is worthwhile to mention that some of the extensive rust zones that were identified from ASTER data correspond to ultramafic dunitic and pyroxenitic rocks with elevated Ni, Cr, Co and platinum group element (PGE) contents, and pentlandite, which was identified using an electron microprobe. It is possible that the Bjørnesund area has a Ni-PGE potential. Rubies were observed at a location in the eastern portion of the Bjørnesund area, close to an amphibolite-anorthosite contact.

These findings indicate that the Bjørnesund Anorthosite-Greenstone belt has the potential to host economic mineral deposits; field work has confirmed that the area is highly prospective, as outlined by qualitative conceptual and quantitative mineral potential multivariable studies done prior to field work.

Key words
Vector to the ore, Ore horizon, Chemostratigraphic relations, Geochemical rock classification, Immobile element ratios, Prospective areas, Remote sensing, Hydrothermal alteration, Pathfinder elements to gold, Multivariate studies, orogenic gold deposit, Bjørnesund Greenstone belt, southern West Greenland

Introduction

The Bjørnesund area is located in southern West Greenland, approximately 40 km North of the Frederikshåb Isblink (Fig. 1A) and approximately 35 km southeast of Fiskeneasset.

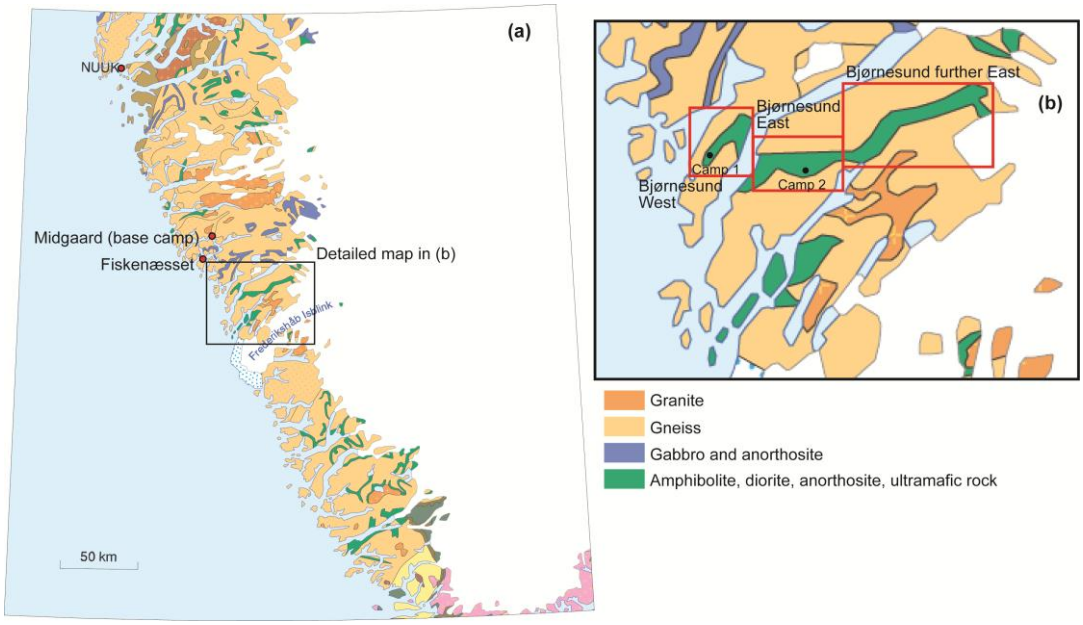

Figure 1. *Simplified geological map of southern West Greenland.* ***A.*** *The Bjørnesund area is located north of Frederiksberg Isblink. The Bjørnesund area, which are in focus for the work presented here, is indicated by the black outlined box.* ***B.*** *The Bjørnesund area can be further divided into Bjørnesund West, Bjørnesund East and Bjørnesund further East (see red outlined boxes). The length of the Bjørnesund Greenstone belt is about 50 km long.*

Samples enriched in gold from the central part of the Bjørnesund East area (Fig. 1B) were reported by NunaOil A/S and GGU in the 1990s (Erfurt 1991, Heilmann 1997, Heilmann 1998) but no work or gold mineralisation have been reported from the Bjørnesund West area prior to the field work in 2009. Little exploration was carried out in the Bjørnesund Fjord after the 1990s. NunaMinerals A/S engaged in limited prospecting in the central part of Bjørnesund East area in 2006, but dropped the licence in 2007 because their 2006 field work did not reveal any additional gold mineralisations (NunaMinerals 2006). The work by NunaOil A/S and NunaMinerals A/S concentrated primarily in the central part of the Bjørnesund East area and the area outside seems to have seen very little to no exploration.

The main focus area, selected for the field work in 2009, was the Bjørnesund West area (Fig. 1B). The selection was based on both qualitative empirical evaluations of the areas by the authors and neural network mineral potential mapping for gold potential (see Stensgaard *et al.* 2012). Also results from processed ASTER (Advanced Spaceborne Thermal Emission and Reflection Radiometer) remote sensing data identified several interesting alteration anomalies in the Bjørnesund Fjord area. These anomalies were also followed up and investigated during the field work.

Selection of target area

The Bjørnesund area was, selected for follow-up prior to the field work based on an evaluation of the results from studies that included both qualitative and quantitative approaches to the favourability for gold in entire southern West Greenland. The approaches are:

- Experience- knowledge-derived qualitative interpretation of geological domains/rock units and mineral potential based mainly on stream sediment geochemistry distribution.
- Quantitative artificial neural network analysis of stream sediment geochemistry distribution, aeromagnetic data, and lineaments extracted from aeromagnetic data, and distribution of known supracrustal-mafic rock units.
- Quantitative unsupervised analysis of stream sediment geochemistry distribution for identification of linear and non-linear relationships in datasets (self-organising map techniques) related to gold potential.

Description of this work can be found in Stensgaard *et al.* (2012). The authors evaluated the results of this work, taking into consideration also the work presented in Stensgaard (2008) and Stensgaard et al. (2006a, b) on the gold potential in the Nuuk region and the historical data and company reports from entire southern West Greenland, when the selection of the Bjørnesund area were made.

The Bjørnesund area was chosen from this evaluation and assessment because:

1) Previous work record indications of gold in parts of the central Bjørnesund East area.
2) Evaluation of the results in Stensgaard *et al.* (2012) indicates that gold potential exists in parts of the Bjørnesund area that not previously had seen focused work.
3) Remote sensing work supervised by the authors indicated several high anomalous Fe^{3+} zones that might be related to hydrothermal zones enriched in iron.
4) Based on the described geology of the Bjørnesund area, both regional and detailed, the authors found that favourable settings for a gold mineralising system were present.

The Bjørnesund area also provided a good study area as other work and mapping by GEUS were planned to be carried out in the area alongside fieldwork carried out as part of this project.

Mineral potential mapping for gold

Two examples on the mineral potential mapping for gold presented in Stensgaard (2012b) are shown in Figure 2.

Statistical analysis of data from the Nuuk region has previously shown that that gold mineralisation are characterised by high Ni/Mg-ratio in the stream sediment data (Stensgaard 2008, Stensgaard et al. 2006a,b). Areas with similar high Ni/Mg areas also occur in the

Bjørnesund West and East areas (Fig. 2A). This result, together with the qualitative assessment of other geochemical elements from the stream sediment geochemistry distribution (see Stenfeldt 2012), indicate a potential for gold in the Bjørnesund area with the highest Ni/Mg-ratio found outside the central Bjørnesund East area which were the only area where gold discoveries previsouly had been reported (Erfurt 1991, Heilmann 1997, Heilmann 1998, NunaMinerals 2006).

Artificial neural network analysis has been used for mineral potential mapping (Fig. 2A–H, see Stensgaard 2012b). The neural network analysis is based on 46 training points, where each point represents a 200×200 m area in the central Nuuk region in which one or more rock samples have yielded more than 1 ppm Au. The training area for the neural network is defined as the region surrounding the training points. Different datasets covering the training area are then analysed by the neural network and the characteristics of the training points are learned. After that the neural network are shown similar type of datasets that covers a simulation area, which in this case covers the entire southern West Greenland. The neural network used the learned characteristics of the training points and outline areas that have similar characteristics in the entire simulation area. The more similar the characteristics are according to what the network have learned, the higher score. As the training points represents areas with gold mineralisations the score can be said to reflect favourability for gold mineralisation (or environments that have similar characteristics as environments with known gold mineralised sites). The western Bjørnesund is being outlined as falling within the top 3% to 4% most favourable area for gold by the neural network analysis of stream sediment geochemistry distribution of As, Cs, Rb, Sb and U, lineaments mathematically derived from processed total magnetic intensity field data and distribution of supracrustal rock units. The top 3% and 4% favourable area of entire southern West Greenland equals 1296 km^{2}and 1727 km^2 respectively out of the 43.187 km^2 analysed (entire southern West Greenland analysed; the simulation area). Favourability refers to that the results of the analysis predict that the data signatures in the Bjørnesund area resemble data signatures of the gold mineralised areas/environments (the training points) in the Nuuk region.

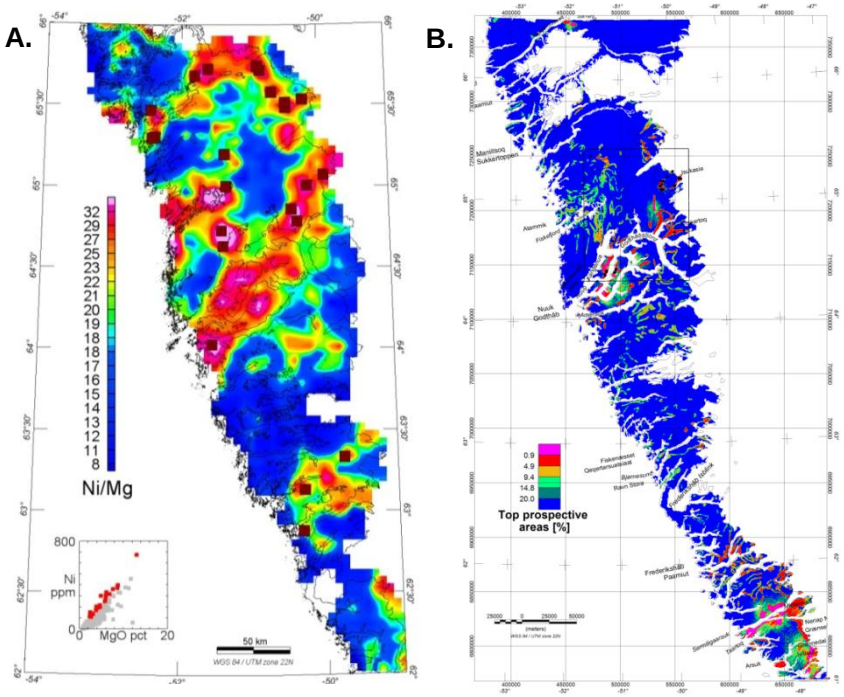

Fig. 2 continues on next page

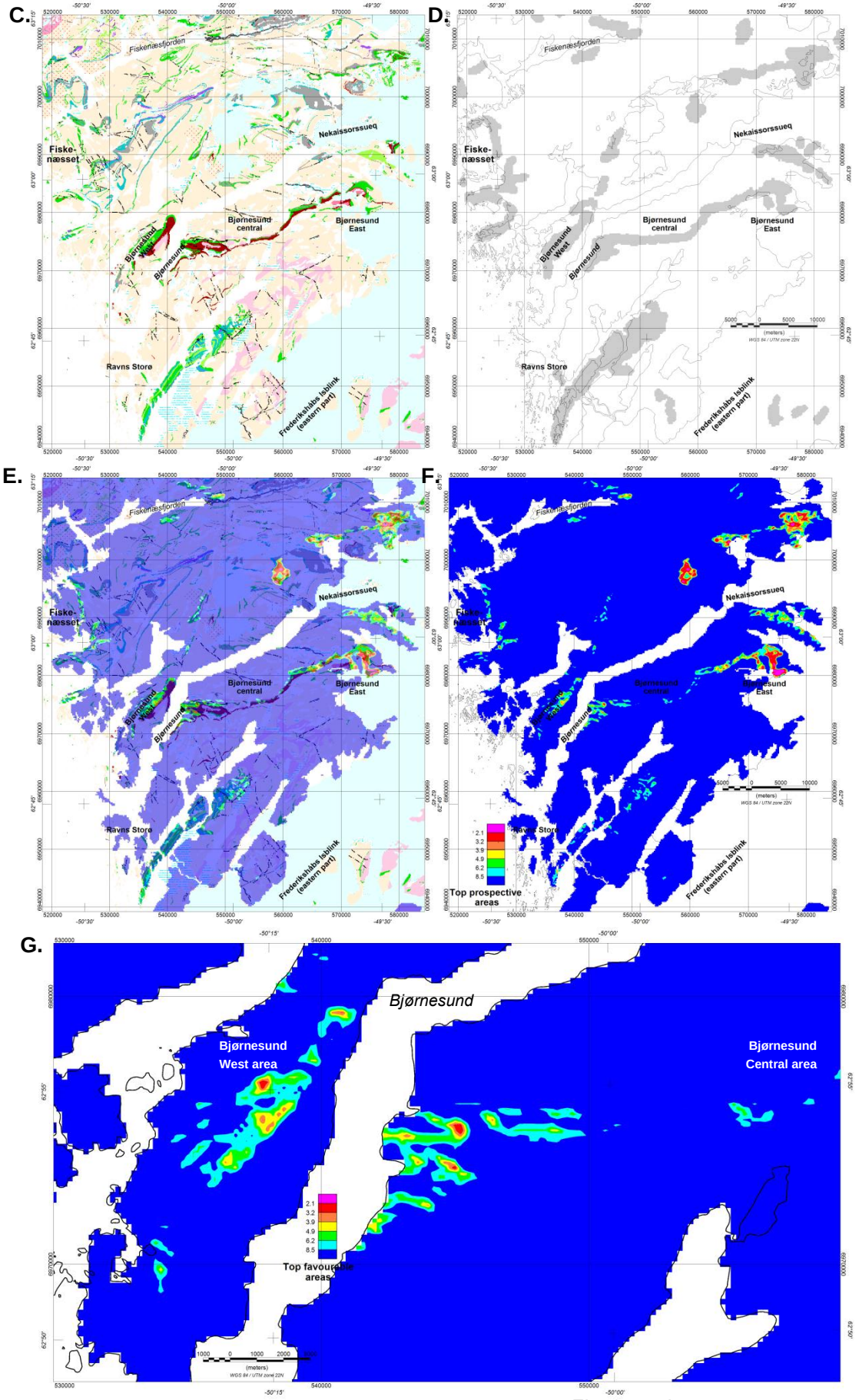

Fig. 2 continues on next page

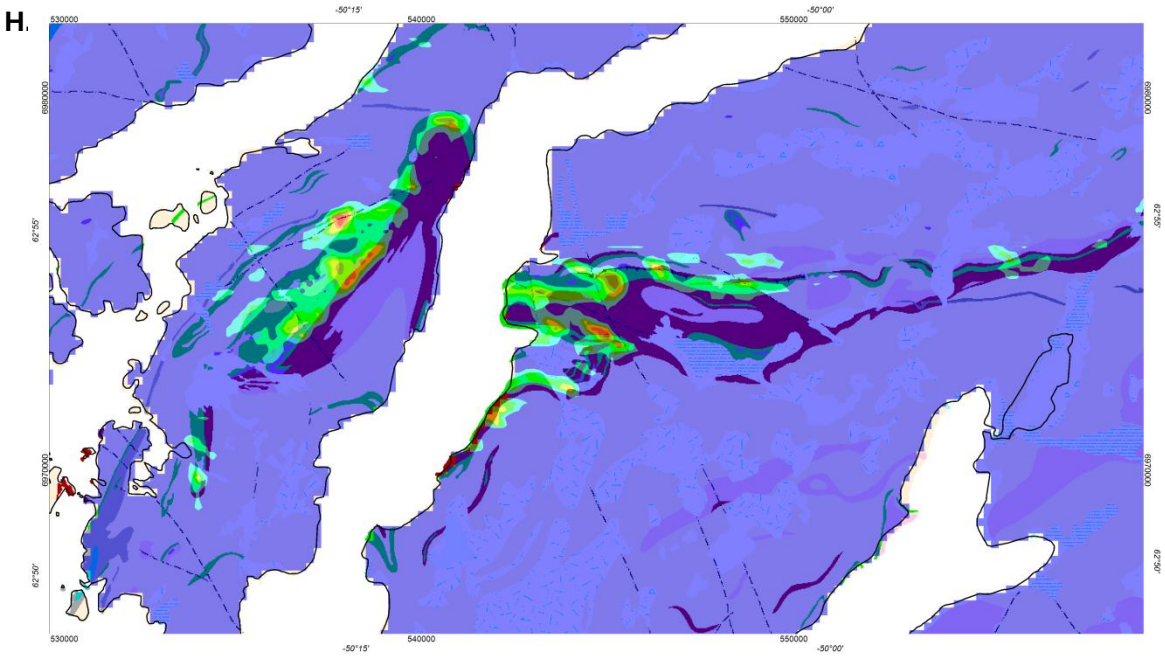

Figure 2. ***A.*** *Map showing the distribution of nickel and magnesium as shown by the Ni/Mg ratios from a large number of analysed stream sediment samples. Areas with high Ni/Mg ratios indicate highly prospective areas with respect to gold mineralisation (Stensgaard 2011, in Kalvig and Thorning, 2011, Stensgaard 2008).* ***B.*** *Neural network analysis for gold favourable areas in entire southern West Greenland based on a combination of As, Cs, Rb, Sb and U stream sediment geochemistry, lineaments and rock unit distribution plotted semi-transparent on top of the geological map. The resulting favourability is shown in 5 intervals.* ***C.*** *Geological map of the Bjørnesund – Fiskenæsset area. Please refer to Keulen et al. 2010b for a legend.* ***D.*** *The supracrustal and mafic units (plus a buffer zone of 600 m that were applied to the outline of all the extracted rock units) that were used as input to the neural network analysis of stream sediment geochemistry, lineaments and rock unit distribution.* ***E.*** *Top 8.5% most favourable areas (in 7 coloured intervals; see legend in F.) for gold according to the neural network analysis of As, Cs, Rb, Sb and U stream sediment geochemistry, lineaments and rock unit distribution plotted semi-transparent on top of the geological map.* ***F.*** *as E. but not in transparent colours.* ***G.*** *As in E but here enlarged for the Bjørnesund West and Central Area.* ***H.*** *As in G but here transparent and with scale 1:100 000 geological map plotted beneath (Keulen et al. 2010b). Figures in 2A–G are from Stensgaard (2012b).*

Results of processed ASTER data

ASTER remote sensing data was collected and interpreted prior to field work by Yong Chen, a GEUS visiting scientist in 2009 who is presently at the Shanghai Institute of Geological Survey. This work was done at GEUS and at the Institute of Land Resources and High Techniques, China University of Geosciences, Beijing.

It is known from other studies that high anomalous Fe^{3+} levels picked up by processed ASTER data can correspond to rust zones. Such rust-zones are formed by the weathering of rock formations that are high in iron. It is important to follow up on these rust zones; gold associated with hydrothermal alteration zones enriched in iron has been reported in several

localities in Greenland, such as the Qussuk area, in the Godthåbsfjord north-west of Nuuk (Fig. 1A). Gold in the Qussuk area is hosted in quartz-veins that are enveloped by pyrrhotite (Schlatter and Christensen 2010). However, rust zones are not diagnostic for gold occurrences; a number of rust zones in Greenland occur because the primary chemistry of the rocks is elevated in iron and weathering of such iron-rich rocks caused rust zones.

ASTER data for the areas immediately east and west of the Bjørnesund Fjord was analysed, and the results of ASTER data modelling were superimposed to the regional geological map (Fig. 3).

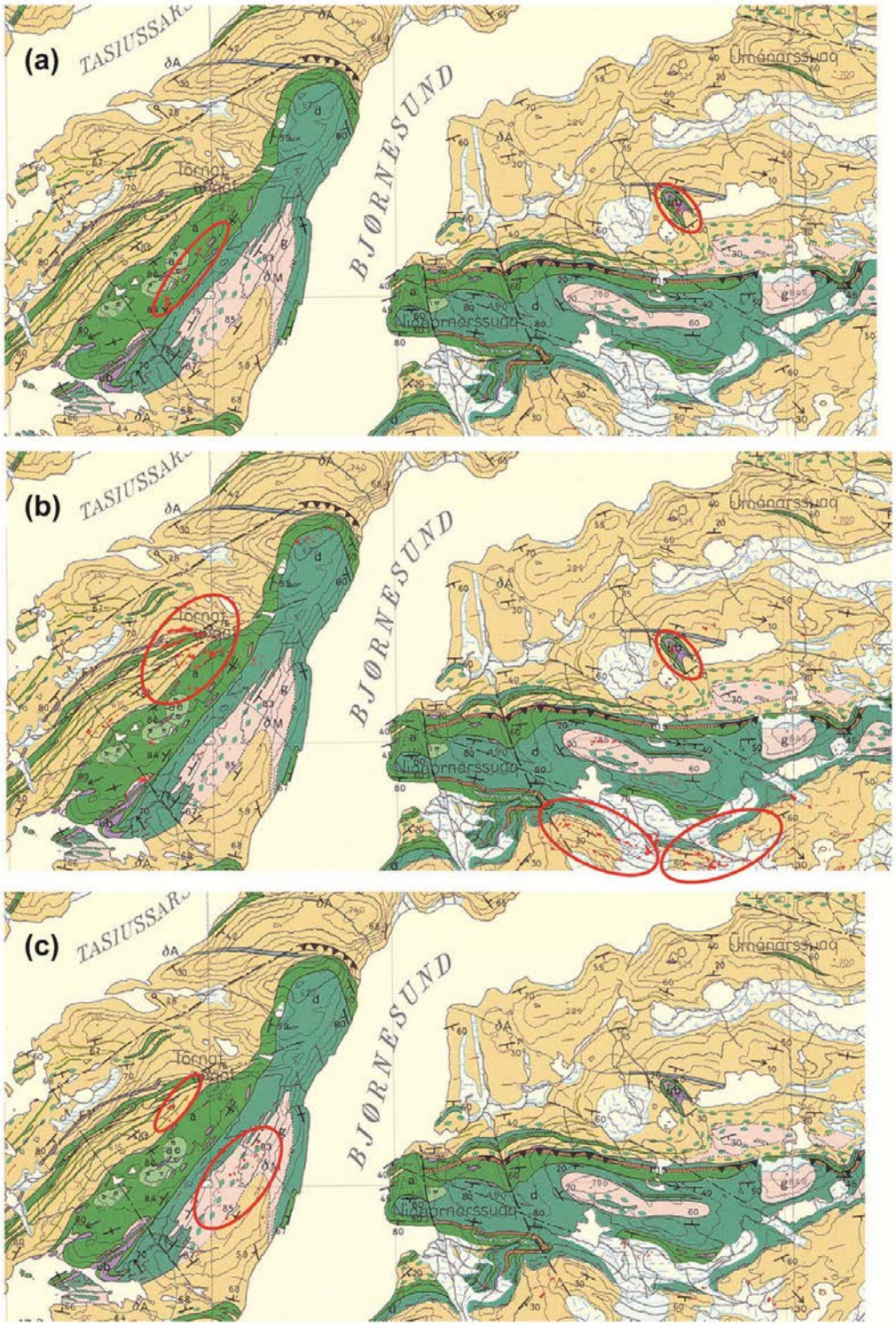

Figure 3. *Interpretation of ASTER remote sensing data and geological map of the Bjørnesund West and Bjørnesund East areas modified from Escher (1976).* ***A.*** *Red pixels show areas where anomalous levels of Fe^{3+} were detected.* ***B.*** *Red pixels show areas where anomalous levels of Fe^{3+} and Mg-OH were detected.* ***C.*** *Red pixels show areas where anomalous levels of Al-OH were detected. (A., B. and C.). Red ellipsoids point towards areas where anomalous levels of elevated Fe^{3+} in A.; Fe^{3+} and Mg-OH in B. and Al-OH in C. occur. For legend see map sheet Bjørnesund 62V.1 NORD, 1:100 000.*

Red pixels on Figure 3A show areas where anomalous levels of Fe^{3+} were detected and it is interpreted that these anomalies correspond to rust zones. Red pixels on Figure 3B show areas with anomalous levels of Fe and Mg-OH^{+}. Such zones possibly correspond to rocks that are rich in hornblende, epidote, biotite and chlorite. Red pixels on Figure 3C show areas where anomalous levels of Al-OH were detected and this anomaly could have been caused by rocks rich in muscovite and illite. It will be shown in a later section of this report that zones with elevated Fe^{3+} as detected from the ASTER data (Fig. 3A) correspond to extensive rust zones. Checks on the ground revealed that these rust zones are only slightly elevated in gold. Field work also showed that these rust zones are caused by the weathering of rocks that were originally rich in iron. Based on these observations, we think that ASTER data is an excellent tool for pinpointing areas where rust zones occur; whether these areas are associated with gold or not needs to be further evaluated by doing field work and geochemical sampling.

Geological setting

Relatively little work was reported from regional studies of the Bjørnesund area (Pulvertaft 1972, McGregor and Friend 1992), whereas the geology of the Fiskenæsset complex which is located north-west of Bjørnesund was described in more detail (Windley *et al.* 1973, Myers 1985).

Appel (1992a) and Erfurt *et al.* (1991) evaluated the mineral potential of the greater Bjørnesund Fjord area with particular focus on possible gold mineralisations. In another work, Appel (1992b) reported the occurrences of tourmalinite associated with hydrothermal alteration zones in the Bjørnesund area. This is interesting because the tourmalinite-gold association has been documented elsewhere, such as the northern Territory of Australia (Plimer 1988).

The simplified geology of the Bjørnesund greenstone belt is shown on Figure 1B and 3A. The greenstone belt is about 50 km long and a few hundred meters to three km wide and mainly comprises amphibolite and quartz-dioritic gneiss (Fig. 1B). The greenstones are bordered towards the north and the south by tonalite-trondhjemite-granodiorite (TTG) gneisses that are interpreted to have been intruded into the greenstones. Sheets of leucogabbros, gabbros and anorthosite are interpreted to have been intruded into the amphibolites of the greenstone belt (Keulen *et al.* 2010a). Finally late granites intruded the sequence of quartz-diorite amphibolite- and anorhosite-gabbro.

Keulen *et al.* (2010 and 2011) provide a structural interpretation of the Bjørnesund area and suggests that the rock package of quartz-diorite, amphibolites and gabbro-leucogabbro-anorthosites and gneiss were affected by F1 folding into a isoclinal synform and F2 folding. The F2 folding has an E-W trending fold axis in the Bjørnesund East area (Fig.3A) and the F2 folding is associated with thrusting that in turn caused shearing with only minor displacement. Late granites then intruded the core zones of the F2 folds. Finally an F3 folding that is trending NNW-SSE slightly bent the regional foliation and has ultimately caused a stair-case-like appearance of the Bjørnesund anorthosite-greenstone belt (Fig. 1B).

Field work and analytical methods used

Field work started and ended from a remote base camp located in Midgaard, about 15 km north-east from Fiskenæsset (63° 13.6242' N and 50° 34.3150’ W; Fig. 1A). The base camp provided services to the nine teams which were carrying out geological investigations in the area roughly located North and South of the base-camp.

The field team number 7 (see "Field Instructions and Standards 2009") comprising Yong Chen (Shanghai Institute of Geological Survey, China; initials: cyo) and Denis Martin Schlatter (GEUS; initials: dms) carried out geological field work in the Bjørnesund area from two camps between June 30, 2009 and July 13, 2009.

Camp one (Fig. 1B) was located in the Bjørnesund West area, ~29 km south-east of Fiskenæsset (62° 54.2910’ N and 50° 16.6452’ W; 393 m above sea level) from June 30 to July 4. Camp two (Fig. 1B) was located in Bjørnesund east area, ~39 km south-east of Fiskenæsset (62° 53.1354’ N and 50° 2.2620’ W; 552 m above sea level) from July 4 to July 13.

Helicopter supported geological reconnaissance was conducted on July 9 in the eastern-most extension of the Bjørnesund greenstone belt with four reconnaissance stops (In some reports this area is also referred to as "Bjørnesund further East"). A number of outcrops that are located in the Bjørnesund West and East areas and that were difficult to access by walking were visited during a helicopter reconnaissance on July 11 and sampling was carried out at two reconnaissance stops. The first reconnaissance stop was made at 62° 54.9840’ N and -50° 5.8188’ W, 163 m above sea level, within the Bjørnesund East area. The second reconnaissance stop was made at 62° 54.7776’ N and -50° 14.9214’ W, 565 m above sea level, within the Bjørnesund West area.

Geological field work was supplemented by the use of hand-held PDAs which were employed to digitally capture the geological field observations (Schlatter *et al.* 2010 and references herein). The digitally captured field data can be found in Appendix A.

The target area that was selected for field work in 2009 was previously mapped in detail by several geologists in the 1970s (Tomas 1970; Pulvertaft 1972). Because high quality geological mapping was already completed it was not necessary to map the area in detail, and the field work by GEUS in 2009 consisted of detailed logging of a cross-section through a gold-mineralised system. Furthermore the earlier completed mapping by Tomas (1970) and Pulvertaft (1972) was complemented by detailed sampling of all present rock types and of the hydrothermal alteration zones. This sampling was done in order to document the geochemical variation of the rocks and the alteration types. Furthermore rock, stream and scree sediments were sampled with the purpose of evaluating the gold potential of the area. It has been shown from earlier studies in southern West Greenland (Schlatter & Chrisensen 2010) that sediment sampling is very useful in the evaluation of the gold potential of an area and to distinguish between sub-areas that could potentially host gold mineralisations and barren sub-areas.

The detailed work in this report focusses on the precise description of the host rocks of a known gold mineralisation in the Bjørnesund West area and on the description of the associated hydrothermal alteration. This is achieved by the detailed description of a 30 m long profile across the tectonostratigraphic sequence. This surface profile was mapped in detail by applying the graphical logging technique (McPhie *et al.* 1993) and by detailed sampling of 15 rocks over the profile.

Other sampling aimed to cover a larger area and to test this area for potential gold mineralisations and to achieve better ideas about the mineralogical and geochemical characteristics of these areas. In summary, the field work carried out in 2009 comprised sampling of 116 rock and 56 sediment samples. Although most of the sampling was done by Team 7 (dms and cyo), some additional rock and sediment samples were provided by other GEUS teams that visited the area in the summer of 2009 on the same expedition, including team 1 (Thomas Kokfelt; initials: tfk), team 2 (Nynke Keulen; initials: ntk) and team 3 (Vincent van Hinsberg; initials: vivh) ("Field Instructions and Standards 2009"). Details of the sampling done by teams 1, 2 and 3 are described in appendix D.

Rock sample preparation and analysis

Rock samples were sent from the base camp to GEUS in Copenhagen where a representative portion of the samples weighting on average ~900 grams (appendix D) was selected and sent to Actlabs laboratory in Ontario. Actlabs then crushed and milled the rock using mild steel equipment (Actlab's code RX2) to avoid any type of contamination of the sample.

The powder was then analysed for the major elements, trace elements, rare earth elements and gold included in Actlab's package "4Lithoresearch and 4BINAA". In addition to Au, the following elements and element oxides were analysed: SiO_2, TiO_2, Al_2O_3, Fe_2O_3, MnO, MgO, CaO, Na_2O, K_2O, P_2O_5, Cr, Ba, Cu, Pb, Zn, Ag, As, Sb, Bi, Tl, V, Ni, Co, Sc, Mo, Sn, W, Ga, Rb, Sr, Cs, U, Hf, Ta, Th, Be, Nb, Y, Zr, La, Ce, Pr, Nd, Sm, Eu, Gd, Tb, Dy, Ho, Er, Tm, Yb, Lu, Br, Ir, Se, Ge, In and LOI (see appendix C for details about the analytical methods used by Actalbs and final reports for work orders A09-5687 and A09-7612).

Rock samples that predominantly comprised quartz-veins were only analysed for gold. Some selected rocks were also analysed for the platinum group elements (PGE).

The quality of Actlabs's analyses was monitored by inserting two GEUS reference samples (Disko-1; samples 508450 and 508451; Appendix D). More details about the GEUS reference sample Disko-1 and the quality control carried out by GEUS can be found in Szilas *et al.* (2011).

Five rock samples were analysed by Acme Labs for major elements, trace elements, rare earth elements and gold (Appendix C).

The lithogeochemical data of the rock samples were recalculated to a volatile free basis as such normalization of the data to 100% facilitates geochemical interpretations (Appendix F; for details of normalization see Appendix 5 in Schlatter, 2007).

Thirty-six polished thin sections were prepared (Appendix D) and preliminary mineralogical studies were carried out, mainly in order to select representative samples for electron microprobe analyses (Appendix J).

The mineralogical studies were done with a Zeiss “Axioskop 40” microscope in transmitted and reflected light, and the electron microprobe analyses were made using a JEOL JXA-8200 Superprobe at the Geological Institute in Copenhagen. An accelerating voltage of 15kV, a focused beam diameter with a cup current of 15 nA, and counting time of 10 seconds on the peak and the background were used to analyse for SiO_2, TiO_2, Al_2O_3, FeO as Fe total, MnO, MgO, CaO, Na_2O, K_2O and Cr_2O_3 in all samples, and NiO and ZnO in some samples (see Appendix J). Natural and synthetic oxides and silicates were used as standards and calibrations were performed on a routine basis. Seven polished thin sections (samples 511907-A, 511907-B, 511927, 511950, 511951, 511982, 511993) were selected for microprobe analyses (Appendix D). The microprobe analyses (296) were used to verify the minerals as identified by the optical microscope and to determine the chemistry of the main phases of the Bjørnesund rocks (Appendix J).

Sediment sample preparation and analysis

Sediment samples were sent from the base camp to GEUS in Copenhagen where the samples were dried at ambient room temperature for several days. Fifty-six sediment samples averaging ~200 grams each where then sieved using a 0.180 mm sieve and the finer-grained-fraction was sent to Actlabs laboratory in Ontario (the sample protocol summarizing the process of the treatment of the sediment samples is given in appendix E). Actlabs then analysed the fraction for Au, Ag, Al, As, Ba, Be, Bi, Br, Ca, Cd, Ce, Co, Cr, Cs, Cu, Eu, Fe, Hf, Hg, Ir, K, La, Lu, Mg, Mn, Mo, Na, Nd, Ni, P, Pb, Rb, S, Sb, Sc, Se, Sm, Sn, Sr, Ta, Tb, Th, Ti, U, V, W, Y, Yb, Zn utilizing their INAA, MULT INAA / TD-ICP and TD-ICP methods (the raw data can be found in Appendix C; and the compiled data are in Appendix D).

Rock samples analysed for geochronology (zircon U-Pb ages)

For the samples 511932, 511945, 511983 and 511994 U-Pb ages (^{207}Pb-^{206}Pb) ages were determined from zircons. In this report the ages of these four plutonic rocks were used to better constrain the lithological setting of the Bjørnesund East area; details of the analytical work done on these four samples are given in Kokfelt *et al.* (2011).

Samples of dykes for potential geochronological dating

Four mafic dykes were sampled and sent for geochronological dating. These analyses were done by M. Nilsson and A. Schersten at Lund University, Sweden. Samples 511908 (locality 09DMS013), 511930 (locality 09DMS048), 511931 (locality 09DMS049) and 511991 (locality 09DMS122) were collected from one location in the Bjørnesund West area and three locations in the Bjørnesund East area (Appendix H) with the purpose of obtaining U-Pb baddeleyite ages of these samples. To date, sample 511930 (from Bjørnesund East) has successfully been processed and separated for baddeleyite, and geochronological analyses are pending.

Samples 511908, 511931 and 511991 were too fine grained to yield any baddeleyite using the currently available separation techniques, however future separation techniques might be improved enough to allow for baddeleyite separation and U-Pb analysis despite the fine grain size of the samples. The four samples remain in Lund for future analysis and possible further processing (personal communication, M. Nilsson).

Digitized detailed geological map from the Bjørnesund West and Bjørnesund East areas

The main focus of this study was concentrated on the areas located immediately west and east of the Bjørnesund Fjord (Figs. 1B and 3). The original geological field maps compiled by Pulvertaft and Tomas covering these areas were digitized and re-compiled (Fig. 4).

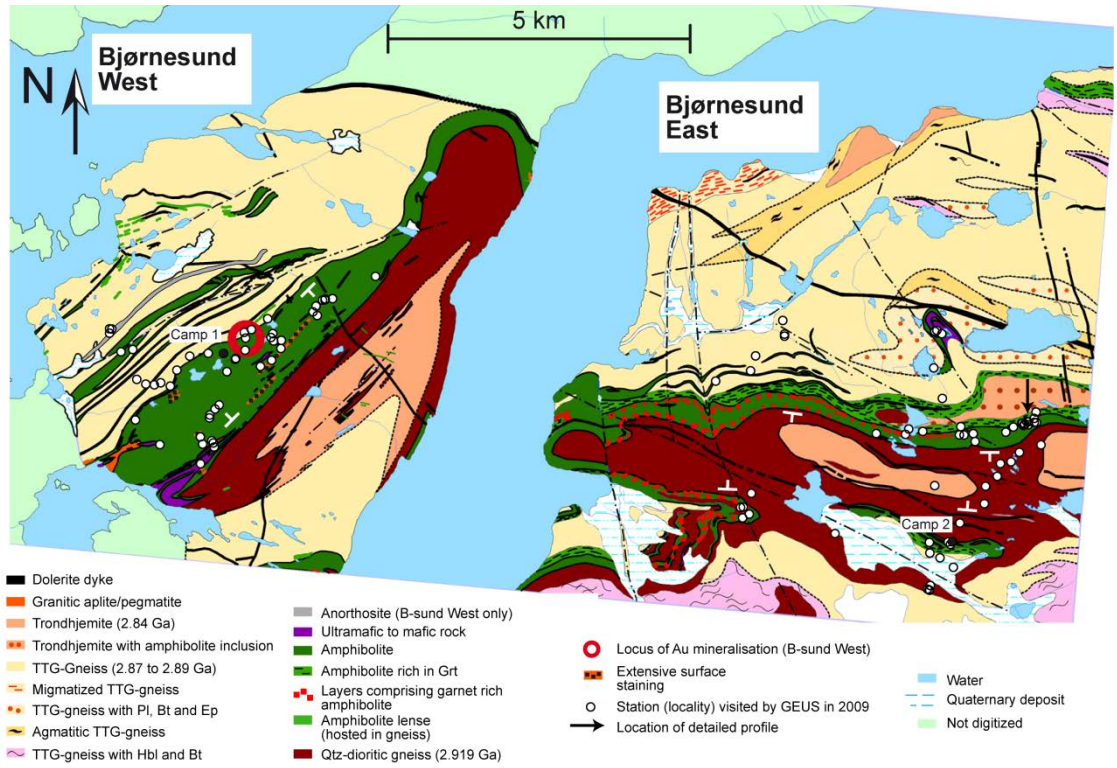

Figure 4. *A newly compiled, detailed and geo-referenced digital geological map (modified from Escher 1976; map is based on detailed mapping by Pulvertaft in 1972 and by Tomas in 1970). Superimposed to the map are stations (white circles) visited by Denis Schlatter and Yong Chen from GEUS during the field season of 2009.*

The Bjørnesund West area was originally mapped by Pulvertaft in 1970 and 1972 at a scale of 1:20 000. The Bjørnesund East area was originally mapped by Tomas in 1970 and 1971 at a scale of 1:20 000 (Both map sheets were used for the production of the 1:100 000 map sheet “Bjørnesund 62 V.1 Nord”, compiled by Escher in 1976). The newly digitized detailed map of the larger Bjørnesund West and East areas recognises 16 rock types in this area.

The 8 main rock types occurring in the Bjørnesund West and Bjørnesund East areas (around the camps 1 and 2) are:

- **Qtz-dioritic gneiss** (2.919 Ga): homogenous, massive, medium to fine grained gneissic rock comprising feldspar, biotite, minor quartz and rare hornblende. The Qtz-dioritic gneiss occurs in the Bjørnesund West and Bjørnesund East areas. In

the Bjørnesund East area, the Qtz-dioritic gneiss occurs in the core of the F2 anticline fold.

- **Amphibolite**: Extensive portions of the Bjørnesund West and Bjørnesund East areas comprise dark green medium grained massive amphibolite (Fig. 4). The amphibolite typically comprises hornblende, plagioclase, quartz and biotite. Pulvertaft (1972) reported the occurrence of distinct pillow structures in the Bjørnesund West area. Variations of the amphibolite comprise the amphibolite rich in garnet and amphibolite with garnet rich layers. The garnet-rich amphibolite is generally rich in garnet throughout the amphibolite unit whereas the amphibolites with garnet layers only contain zones or layers within the amphibolite that are rich in garnet.

- **Ultramafic to mafic rock:** The ultramafic to mafic rocks range from meter-sized elongated bodies to lens-like bodies that are up to 500 m long and 200 m wide. One of these bodies occurs isolated within the gneisses in the northern part of the Bjørnesund East area (Fig. 4). The ultramafic to mafic rocks comprise pyroxenites, peridotites and dunites. The pyroxenites comprise pyroxene, plagioclases and minor titanite. The dunites comprise predominately olivine, and contain minor Fe-hydro-oxides, chlorite, plagioclases and spinel. Other rocks within this group are best described as ultramafic rocks, and these rocks have a characteristic weathering surface and predominately comprise carbonates, amphiboles, pyroxenes and minor magnetite.

- **Anorthosite:** Anorthosite occurs as whitish, homogenous, relatively small units with smooth surfaces that are hosted in the gneiss in the Bjørnesund West area. The anorthosite comprises predominately anorthite with minor brown mica, quartz, hornblende and epidote. Boudins of gabbro occur within the anorthosite but they are too small to be shown on the detailed geological map (Fig. 4).

- **TTG-Gneiss** (2.87 to 2.89 Ga): TTG-gneisses are widespread in the northern part of the Bjørnesund West and Bjørnesund East areas. The poorly-foliated gneisses are grey and comprise quartz, feldspar, biotite and hornblende. This work is not focused on the TTG-gneisses; only a few gneiss outcrops were visited. It can be seen from Figure 4 that several types of gneiss were distinguished including TTG gneiss, migmatised TTG gneiss, and other variations of gneiss.

- **Trondhjemite (2.84 Ga):** These rocks are granite-like, and comprise quartz, garnet, K-feldspar, plagioclase and biotite. Variants include a trondhjemite with amphibolite inclusions that crops out in the northern part of the Bjørnesund East area (Fig. 4).

- **Granitic aplite/pegmatite:** The granitic aplite and pegmatites crosscut the stratigraphy and are of various thickness. A 700 m long and 100 m wide unit of lineated granite is seen in the western part of the Bjørnesund West area; it is unclear if this unit comprises granitic pegmatite or trondhjemite. In the Bjørnesund East area, several multi-meter-thick aplite/pegmatite units occur within the amphibolites.

- **Dolerite dykes** are widespread in the area and crosscut all the other rock units. The dykes range from fine- to medium-grained and vary from a few centimetres to 50 m in width (Pulvertaft 1972). The dykes sampled in this study are a few meters to up to 10 m thick and predominately contain pyroxene.

In the next chapter of this report the main rock types encountered during field work from two field locations (camps) are described.

Field work carried out in the area of Camp 1

The Bjørnesund West area is located between UTM 6980151 and 6971251 (northing) and UTM 532163.6 and 541633.9 (easting); (Fig. 4). Camp 1 was set up roughly in the centre of the NE-SW trending greenstone belt of the Bjørnesund West area (Fig. 4; Appendix B, IMG_1762).

The Bjørnesund West area was selected for field work because of several indications from the multivariate studies that the area was favourable to host gold mineralisations (see earlier section and Figure 2). Because Camp 1 was located in the centre of the greenstone belt it was possible to reach most of the outcrops of the area on foot and to carry out most of the geological field investigations by walking from the camp.

Prior to the field work, the greenstones were selected as particularly interesting for further geological work and were recognized as good targets for gold exploration based on Ni/Mg ratios (Fig. 2). Furthermore, it is known from several other areas in Greenland that gold can be found in Archaean greenstone belts (Schlatter and Christensen, 2010).

Typically the dark green amphibolite seen in the Bjørnesund West area comprises hornblende, plagioclase and quartz and occasional sulphides. Amphibolites occur 200 m east of Camp 1 where they form a steep cliff at locality 09DMS008 (Appendix B, IMG_1756). Foliation of the amphibolites generally strikes in NE direction and is steeply dipping. Some of the amphibolite layers are rusty stained at surface (Appendix B, IMG_1760).

The steep dipping of the outcrops near Camp 1 (locality 09DMS008 and 009) is caused by intense shearing and results in a prominent shear zone. This shear zone has transposed the original foliation of the rocks into the orientation of the shear zone. Sheeted and foliation parallel quartz veins up to 50 cm thick occur, but they are not gold mineralised at the sampled locality (Appendix B, IMG_1763). A several tens-of-metre wide shear zone was studied at 50°16.2'W and 62°54.4'N at 555 m elevation above sea level at locality 09DMS011 about 450 m north-east from camp 1 (Appendix B, IMG_0536; IMG_1766). This shear zone is trending NE-SW and steeply dips 80 degrees towards SE. The shear zone can be followed over several hundred-of-metres along strike. In detail, this shear zone contains a 50 cm yellow-brownish, rusty-stained amphibolite, which hosts parallel quartz-carbonate veinlets containing minor feldspar, mica and iron oxyhydroxides.

Chip samples over 50 cm of the rusty stained amphibolite yield 569 ppb Au (Minex 35, December 2009). The amphibolite comprises hornblende, minor pyroxene and large garnet porphyroblasts of up to a few centimetres in diameter. A unique feature of these amphibolites is the occurrence of mm-thin and cross cutting veinlets comprising quartz and iron oxyhydroxides. We suggest that this unusual mineral assemblage (quartz and iron oxyhydroxides) was caused by hydrothermal alteration likely associated with the gold mineralisation event. A similar amphibolite to the one which hosts 569 ppb gold is located 1.5 km towards SW and yields 31 ppb over about 10 m chip sample profiles. The description and the mineralogical assemblages of this gold-enriched and altered shear-zone will be provided in a later section of this report.

Other shear zones, 1.25 km NE from the locality 09DMS011 where the gold was discovered were sampled at the locality 09DMS018 but the amphibolite and a 15 cm thick quartz-vein at that locality were barren in gold (Appendix B, IMG_1781).

ASTER remote sensing data indicated anomalous levels of Fe^{3+} in an area ~1.6 km north-east of Camp 1 (Fig. 3A). This locality (09DMS019) was visited during the field work and it became apparent that the ASTER anomaly is resultant of an extensive rust zone. At locality 09DMS019 outcrops of strongly rusty-stained amphibolite were sampled. After having inspected the field outcrops, it was recognize that some of these outcrops were previously sampled by channel cutting and the literature revealed that these strongly rusty stained rocks did not contain gold (Appel 1992a). This was again confirmed by the sampling done in this report; these amphibolites do not contain gold, although they are rusty-stained at surface. This staining is best explained by the pyrrhotite-rich nature of the amphibolite and the surface weathering of the sulphides which led to rust zones. These rust zones are several hundred meters long and their orientation is roughly parallel to foliation (Fig. 4). Several rock samples of these rust zones were collected and analysed for gold; none of the samples yield gold above the detection limit (2 ppb).

Non-rusty-stained amphibolites that were less affected by hydrothermal alteration were studied at locality 09DMS116 and here the least altered amphibolite comprises hornblende, plagioclase, quartz and minor mica.

Generally the amphibolites in the Bjørnesund West area only show minor petrographic variations; however, intensities of hydrothermal alteration vary. It will be shown in a later section that lithogeochemical methods based on immobile element ratios have allowed for the distinction of seven different primary amphibolites types. Based on this lithogeochemical analysis, a geochemical map was constructed and a chemostratigraphy was established.

Several samples from the localities 09DMS033, 034 and 035 (these localities are in proximity of the locality 09DMS011 were the gold mineralisation was found) were sampled for future microtectonic studies. Such microtectonic investigations will provide additional information regarding the extensive shear zone. These data are important for the characterisation and understanding of gold-mineralised shear zones. A better understanding of this shear zone will help to make future gold exploration more efficient.

As seen from the geological map (Fig. 4), elongated narrow 25 to 50 meter thick units are mapped as anorthosites belonging to the gabbro-leucogabbro-anorthosites units that were described in an earlier section. The anorthosite outcrops were visited and sampled at the locality 09DMS042 and the rocks there are of whitish colour with a smooth surface (Appendix B, IMG_0589). The rocks comprise predominately plagioclase and minor brown mica; minor phases are hornblende, pyroxene and epidote (sample 511927 from this locality was analyzed by Electron Probe Microanalyzer (EPMA), Appendix J). Small gabbro bodies of 1–1.5 m thick occur as boudins within the anorthosite sheet (Appendix B, IMG_0590). They are white to greenish in colour and contain plagioclase and pyroxene.

Several units of mafic to ultramafic rocks lenses occur as lens-shaped greenish and sometimes rusty-stained bodies within the amphibolite sequence. Outcrops of this unit were visited at the locality 09DMS031 ~1.8 km south of Camp 1 (Fig. 4; Appendix B, IMG_0569, IMG_1821). Here a relatively large body of greenish colour rocks with rusty patches crops out. The samples from this outcrop yield ~1000 ppm Cr, with elevated Ni content up to 230 ppm. These basalts comprise predominately amphiboles, and also contain opaque minerals and patchy and stringer-like iron oxyhydroxides. Other rocks belonging to the same body were visited at locality 09DMS029; basalts at this locality have 1310 ppm Ni and 1730 ppm Cr. Other rocks of similar appearance were visited ~900 m northeast of Camp 1 at locality 09DMS015 (Appendix B, IMG_0540). The ultramafic to mafic rocks at this locality are brownish-yellow, contain olivine and pyroxene and yielded 2060 ppm Cr and 1340 ppm Ni.

In summary, the Bjørnesund West area that was visited in the summer of 2009 is dominated by amphibolites containing bodies and slivers of ultramafic to mafic rocks. Some units of the amphibolites are affected by surface weathering which has caused extensive rust zones, but are barren in gold. The most interesting gold occurrences, with gold contents of up to 569 ppb, are found in a hydrothermally altered shear zone.

The amphibolites were intruded by TTG gneisses, which is observed in the western part of the Bjørnesund West area, where small elongated bands of amphibolite remain as relicts in the TTG gneiss. This rock sequence was then affected by F1 folding into an isoclinal synform and F2 folding and was offset by F3 folds as has been described in an earlier section.

In the Bjørnesund West area, 30 samples were selected for lithogeochemical studies. Gold analyses reveal that only 9 rocks contain gold higher than 10 ppb; 7 of these rocks are ultramafic to mafic basalts, and two are from quartz-veins samples (Appendix D). It will be shown in a later section of this report how the rock samples with elevated gold contents together with the gold anomalous sediment samples are used to define areas which are anomalous in gold and in turn are targets for future gold exploration.

Field work carried out in the area of Camp 2

Camp 2 was located in the eastern part of the greenstone belt in the Bjørnesund East area (Fig. 4; Appendix B, IMG_2020; 2040, 2225). Camp 2 was also used to explore the Bjørnesund further East area (the Bjørnesund East and Bjørnesund further East areas are located between UTM 6985728 and 6971803 (northing) and UTM 541880.1 and 576117.3 (easting).

Similar to the Bjørnesund West area, the Bjørnesund East area is dominated by a thick Qtz-diorite gneiss-amphibolite sequence with mafic to ultramafic rocks lenses. This rock sequence was intruded by TTG gneiss. This gneiss forms crops out extensively in the northern part of the Bjørnesund East area. The Bjørnesund East area comprises an anticline structure with elongated granitic bodies in the core of the anticline. The structural evolution of the Bjørnesund East area was summarized by Keulen *et al.* (2010) and has been discussed in an earlier section.

The Qtz-diorite gneiss-amphibolite sequence was studied from outcrops in the eastern part of the Bjørnesund East area (Fig. 4, see "Location of detailed profile"). Here a detailed surface profile was graphically logged about 50 m across the amphibolite sequence (Fig. 5).

Three meter thick amphibolite units immediately above the Qtz-diorite gneiss contain elevated gold, and represent the Bjørnesund East ore horizon (Fig. 5, Appendix G). Because no primary volcanic textures occur, it was not possible to determine the stratigraphic younging direction and accordingly the amphibolite sequence was divided into structural foot wall (FW), ore horizon and structural hanging wall (HW).

The Qtz-dioritc gneiss in the structural footwall is relatively coarse grained, of greenish colour and has a gneissic appearance (Appendix B, IMG_0718). The Qtz-dioritc gneiss comprises plagioclases, hornblende, quartz, biotite and few opaque minerals. The same Qtz-dioritc gneiss was investigated from the southern limb of the anticline from outcrops immediately east of Camp 2 at locality 09DMS127 (Fig. 4). There the grey Qtz-dioritc gneiss (Appendix B, IMG_0749) comprises plagioclase, quartz, hornblende, biotite and minor sphene and chlorite.

From the detailed surface profile (Fig. 5) it can be seen that the ore horizon corresponds to two amphibolites layers (samples 511981 and 511982). These layers comprise plagioclase, hornblende, garnet, biotite and quartz. Similar to the gold mineralized rocks in Bjørnesund West, the rocks from the Bjørnesund East ore horizon also contain small veinlets comprising quartz and oxyhydroxides and patches of oxyhydroxides (sample 511982 was also analysed by EPMA, Appendix J). The structural HW comprises a sequence of about 10 m of amphibolite. The HW amphibolite is lithologically variable, and several distinct horizons are identified. The lithological variations within the amphibolite are primarily a function of mineralogical variations. Some zones are rich in garnet, whereas other zones contain sulphide minerals that have resulted in rust surface staining. Finally some units are thinly layered. These units comprises alternative a few tens of centimetre thick weathered relatively soft amphibolite layers and a few tens of centimetre thick slightly more silicified and conse-

quently less weathered amphibolite. These harder units are also rich in very thin quartz veinlets.

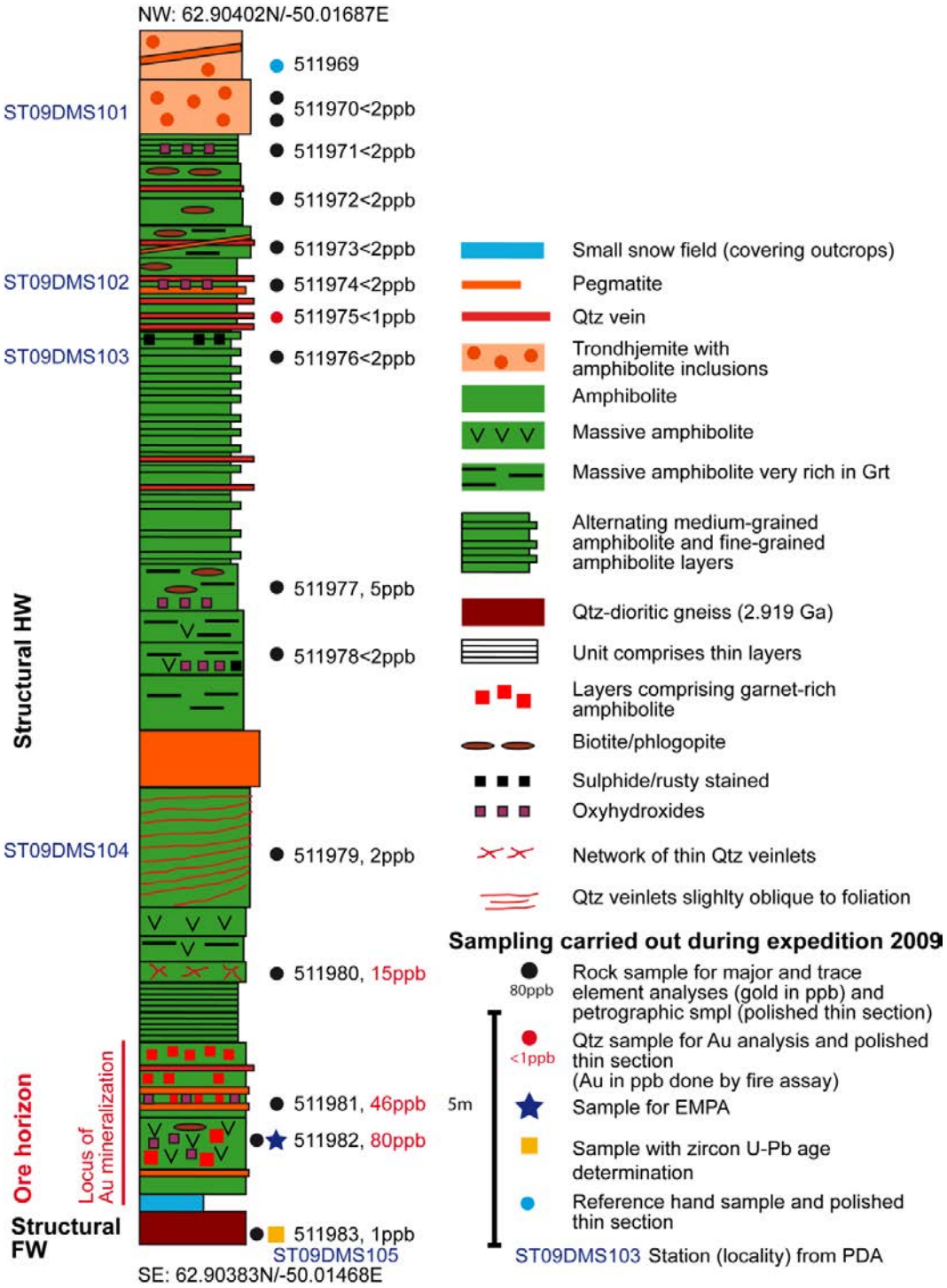

Figure 5. *Simplified tectonostratigraphic sequence of Bjørenesund West based on detailed geological mapping of a surface profile done by Denis Schlatter during field work in 2009. For location of the surface profile see Figure 4. Photographs were taken from each sample station and can be found on Appendix B (IMG_0703_ST_09DMS101_smpl_511969.jpg to IMG_0718_ST_09DMS105_smpl_511983.jpg).*

All amphibolite units contain hornblende, plagioclase and quartz. The quartz veinlets in the lower part of the structural footwall are less than a centimetre in width and oblique to foliation, whereas several quartz veins in the upper part of the structural hanging wall are several centimetres wide.

This tectonostratigraphic sequence is intruded by pegmatites; one pegmatite of the structural footwall is up to 1 m thick. Numerous thinner pegmatites are located in the ore horizon and in the hanging wall (Fig. 5).

Outcrops of TTG gneiss were studied at locality 09DMS112 close to the northern contact of ambhibolite and TTG gneiss. The grey gneiss (Appendix B, IMG_0725) is rich in quartz and feldspar and is crosscut by small 2 to 5 cm wide quartz veinlets.

Relatively large units of mafic to ultramafic rocks are cropping out 3.7 km north of camp, and these up to 500 m long and 200 m wide elongated bodies were described in an earlier section. Sample 511950 is a mafic rock rich in amphibole, pyroxene and plagioclase; minor sphene occurs as inclusions in the pyroxene. Sample 511951 is an ultramafic rock comprising olivine, pyroxene, and minor spinel. Samples 511950 and 511951 were studied by the electron microprobe (Appendix J). Although these rock units are strongly affected by surface weathering and large areas are rusty stained (Appendix B, IMG_1996, IMG_2000, IMG_2015), no gold is associated with these rusty zones. These rocks contain elevated contents of Cr and Ni. The extensive rust zones were recognized from ASTER data modelling by the elevated pixel concentration of Fe^{3+} (Fig 3A). Other ultramafic to mafic rocks were studied 55 m southeast of camp 2 at locality 09DMS126 (Fig. 4). These rocks form elongated bodies, a several hundred meters long and a several tens-of-meters wide. They are of yellowish brownish colour and show a characteristic type of surface weathering (Appendix B, IMG_0748). The rocks mainly contain carbonates, magnesite and amphiboles. These rocks are elevated in Cr and Ni as seen from sample 511993 (Appendix D). The same sample was analysed with the electron microprobe and the Ni bearing mineral was identified as pentlandite (Appendix J, 511993038.bmp).

Outcrops of trondhjemite were studied and sampled at two localities in the Bjørnesund East area. In the central part of the Bjørnesund East area (location 09DMS068), a ridge comprises an elongated body of massive coarse grained light grey coloured trondhjemite about 3.4 km long and up to 700 m wide (Fig. 4). These homogenous rocks expose smooth surfaces (Appendix B, IMG_1978). In the eastern part of the Bjørnesund East area the same trondhjemites were studied at locality 09DMS052 at the contact between the granite and the Qtz-dioritic gneiss (Fig. 4; Appendix B, IMG_0611). There the trondhjemite comprises mainly quartz and plagioclases with minor biotite (some of the plagioclases are slightly altered to sericite). These coarse-grained felsic plutonic igneous rocks comprise predominately quartz and plagioclases with minor biotite. Lithogeochemistry (see later section of this report) confirms that these rocks are trondhjemites.

Field work carried out from reconnaissance stops

A helicopter supported field reconnaissance trip (reco.) was undertaken to pre-selected localities on July 9 with the purpose of inspecting the easternmost extension of the anorthosite-greenstone belt (Figs. 1 and 6) and to carry out sampling for lithogeochemical investigation. This easternmost extension of the anorthosite-greenstone belt was studied at four reco. stops (Fig 6).

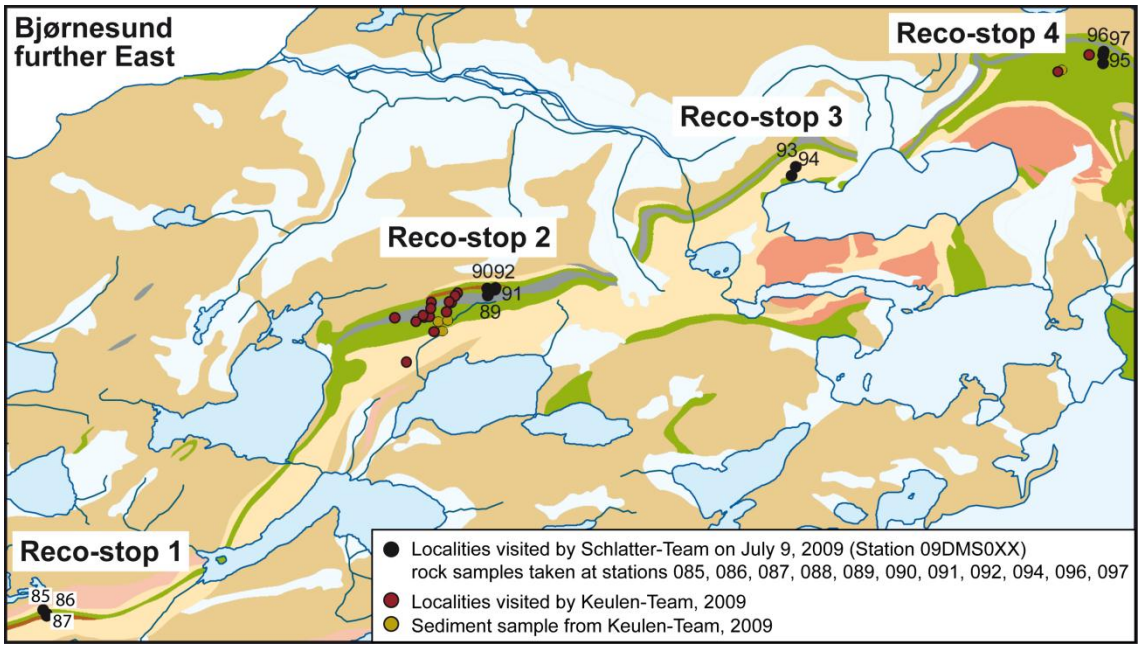

Figure 6. *The map shows locations and sampling carried out in the Bjørnesund further East area where four reco. stops were made by DMS and CYO. Superimposed are the locations visited by another GEUS team (Nynke Keulen and John Schumacher) in the summer of 2009. For legend see map sheet Bjørnesund 62V.1 NORD, 1:100 000.*

Reco. stop 1

The rock sequence TTG Gneiss (Fig 6, location 09DMS085; Appendix B, IMG_0661) – basaltic mica-schist (location 09DMS086, Appendix B, IMG_0662) – basaltic garnet schist (location 09DMS087, Appendix B, IMG_0663) was sampled over a distance of 120 m.

Reco. stop 2

The rock sequence at this reco. stop consists of mafic pyroxene rich amphibolite (Fig 6, location 09DMS088, Appendix B, IMG_0665), whitish anorthosite (location 09DMS089, Appendix B, IMG_0666), basaltic amphibolite (location 09DMS090, Appendix B, IMG_0668) and basaltic garnet schist (location 09DMS092, Appendix B, IMG_0674). Although the field-work reported here concentrates on the assessment of the gold potential in

the Bjørnesund area, it is worthwhile to mention that rubies were observed at the location 09DMS091, near to the amphibolite-anorthosite contact (Appendix B, IMG_0670). The profile studied at the reco. stop 2 is ~200 m long.

Reco. stop 3

The original intention of reco. stop 3 was to make a cross section trough the anorthosite-greenstone belt in the middle part of the Bjørnesund further East area (Fig. 6). Because of very steep terrain at the location, it was not possible to access the contact by helicopter; the closest available landing position was about 350 m SE of the target. A Qtz-dioritic gneiss was sampled at locality 09DMS094 (Appendix B, IMG_0675).

Reco. stop 4

This stop was made to examine and sample the easternmost part of the anorthosite-greenstone belt at two localities (Fig. 6). At locality 09DMS096 a white grey impure anorthosite crops out (Appendix B, IMG_0680) and at locality 09DMS097 a basaltic amphibolite was examined (Appendix B, IMG_0681).

In the limited time available in the Bjørnesund further East area, the only work undertaken was sample collection and basic rock description (Appendix A). It will be shown in the section ‘Lithogeochemistry of the Bjørnesund area’ that the geochemical data from these samples are very useful for the chemostratigraphic interpretation of the entire Bjørnesund area.

Lithogeochemistry of the Bjørnesund area

Chemical rock definition and magmatic affinity of least altered representative rocks

Seventy-three samples were selected for whole rock major and trace element analysis. Samples were screened for hydrothermal alteration based on field descriptions (such as absence of alteration minerals and sulphides) and on geochemical criteria such as low contents of "unusual" elements such as Au, Ag, As, Sb, Bi and W, elements which are typically introduced in the rocks by hydrothermal fluids. The least altered rocks are TTG-gabbro-anorthosites, ultramafic rocks, one dolerite dyke and one Qtz-plagioclase-Hbl rock. Only three amphibolites were identified as least altered whereas the other 40 amphibolites were affected by hydrothermal alteration. Thirty-three samples were recognized as being least altered, whereas 40 amphibolite samples are hydrothermally altered. Only the amphibolite samples are hydrothermally altered; whereas the other rocks although some of them mineralized are thought to be results of orthomagmatic results rather than resulting from hydrothermal alteration.

Rock definition of least altered samples

Major and trace element compositions of the least altered samples are plotted on standard geochemical diagrams to assess rock type. Figure 7A shows that the ultramafic to mafic samples, the gabbro samples, and the least altered amphibolites are of basaltic composition.

Major element oxide composition indicates that the Qtz-dioritic gneisses are andesitic or lie at the boundary between the dacite and basalt fields, the dolerite dyke is of dacitic composition, and the TTG gneisses and trondhjemites are of felsic composition (Fig. 7b.). Figure 7b shows that the least altered Bjørnesund samples are of subalkaline affinity. The plutonic igneous rocks can be further classified into trondhjemite, tonalite, granodiorite, quartz-diorite and gabbro on a diagram based on major element ratios (Fig. 8A and 8B).

Rocks were classified into several main groups in the field: amphibolite, anthophyllite rich rock with sapphirine, dunite, peridotite, phyllite, pyroxenite, schist, serpentinite, and ultramafic rock (appendix, “GanFeld”). All these 13 rocks and are mainly ultrabasic to basic (Fig. 7A and 7b). Samples are also plotted on a FeO+TiO2, Al2O3 and MgO ternary diagram (Fig. 9A), indicating that most samples are basalts and that some plot into the komatiite-field. The rocks can be classified into three distinct groups based on Zr vs. Cr discrimination diagrams: high Mg-Cr-Ni-Co basaltic dunite, high Ti-Zr basaltic pyroxenite and Ni-rich basalt (Fig. 9A). The samples which plotted in the komatiite-field of Figure 9A are classified as high Mg-Cr-Ni-Co basalts in Figure 9B.

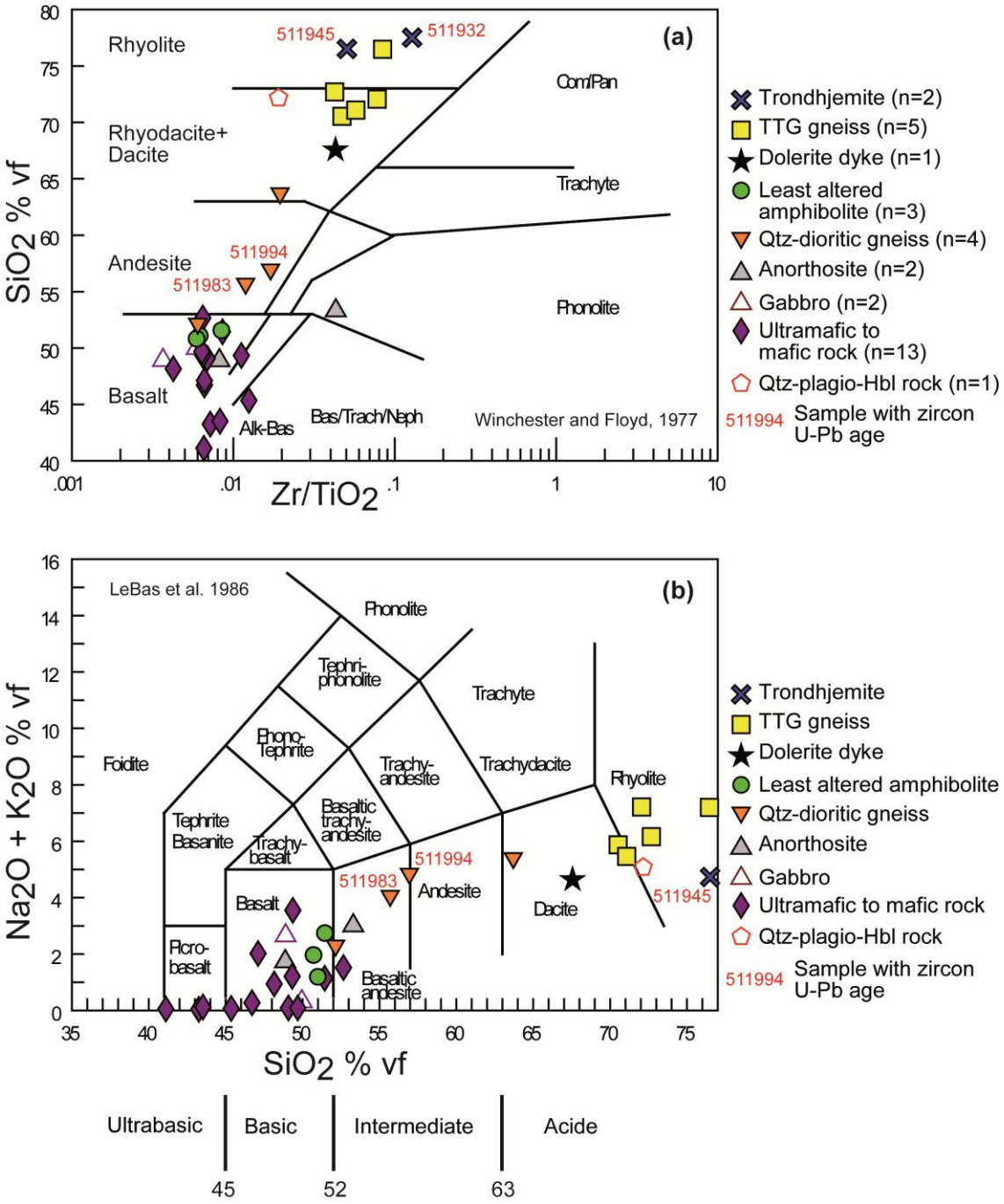

Figure 7. *Chemical classification of least altered samples from the Bjørnesund area.* ***A.*** *Least altered rocks are plotted into the diagram by Winchester and Floyd (1977).* ***B.*** *The same least altered rocks that were shown in A. were also plotted into the diagram by Le Bas et al (1986). TTG and Trondhjemite samples are also plotted in Figure 8. (vf: volatile-free basis, data were normalised after loss on ignition, LOI).*

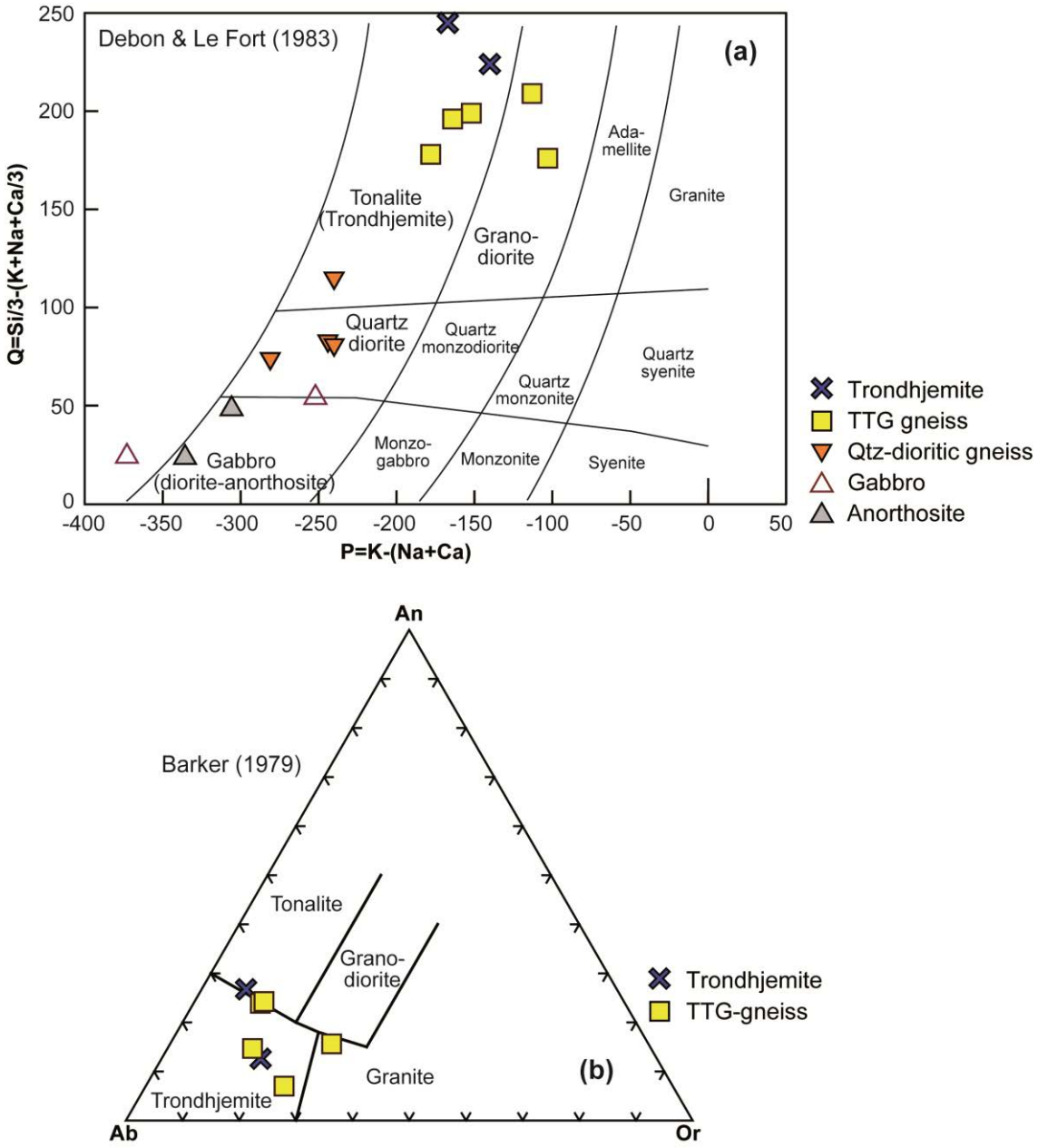

Figure 8. *Classification of the felsic igneous rocks and the gabbro-anorthosite units.* ***A.*** *Samples are plotted into the Debon & Le Fort (1983) diagram and the samples fall into the fields of Tonalite-Trondhjemite, Granodiorite, Quartz-diorite and Gabbro.* ***B.*** *The ternary plot by Barker (1979) is based on the proportions of An, Ab and Or of each sample. The samples from Bjørnesund fall into the Tonalite-Trondhjemite, Granodiorite and Granite fields. Several samples straddle borders between fields.*

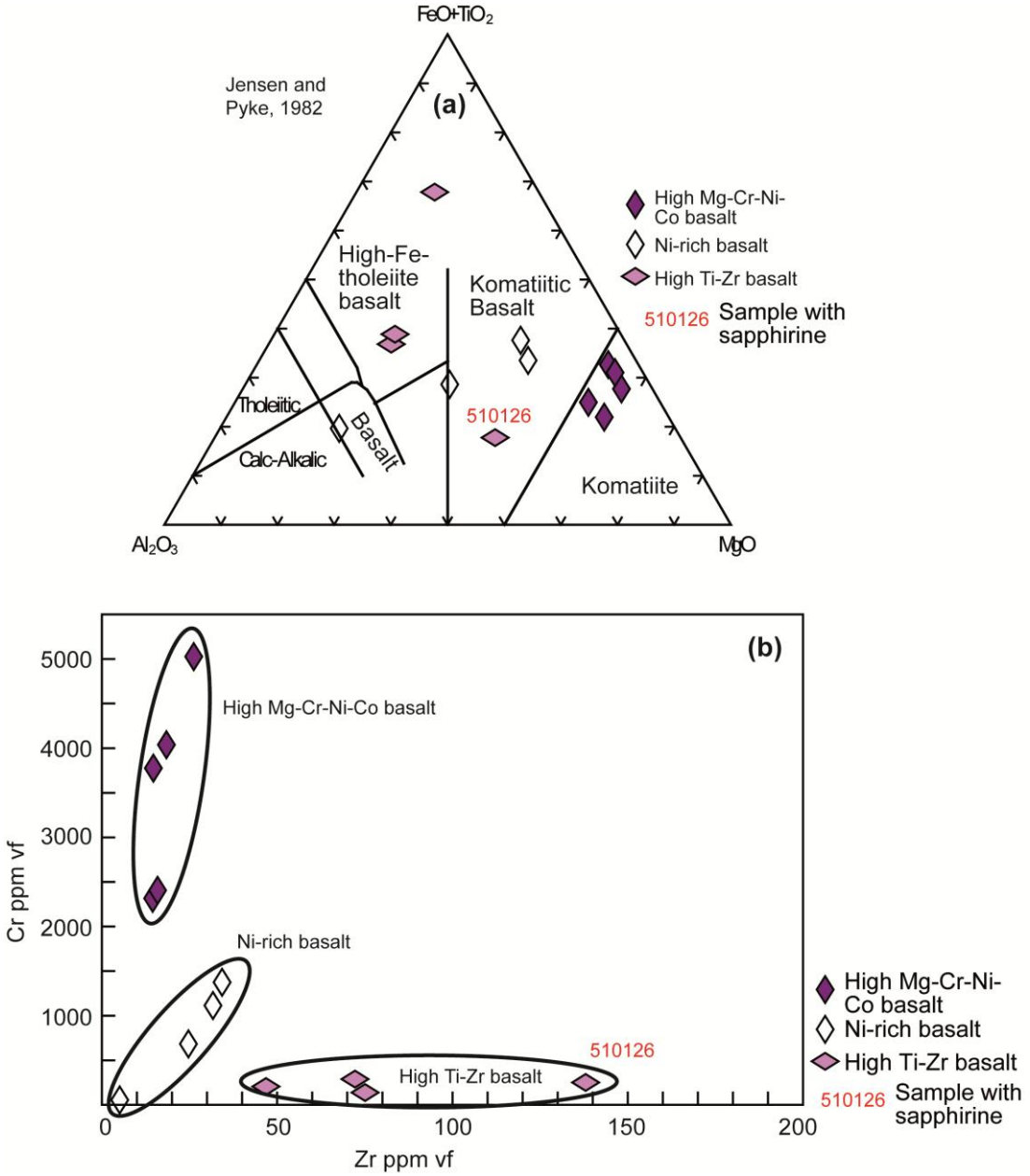

Figure 9. *Classification of the ultrabasic and basic rocks.* ***A.*** *Samples from Bjørnesund fall into the Komatite, Komatitic basalt, high Fe-tholeiite basalt and basalt field in the diagram by Jensen and Pyke (1982).* ***B.*** *The high Mg-Cr-Ni-Co basalt, the Ni-rich basalt and the High Ti-Zr basalt samples fall into distinct groups in a scatter diagram based on Zr and Cr. The fields to discriminate different ultrabasic and basic rocks in this diagram are innovative for this report, but inspired by Pearce (1996). (vf: volatile-free basis, data were normalised after loss on ignition, LOI).*

Magmatic affinity of least altered samples

Samples were plotted on an AFM diagram in order to determine the magmatic affinity of the least altered Bjørnesund samples (Fig. 10A). The majority of samples fall into the tholeiitic field, with the remainder in the calc-alkaline field.

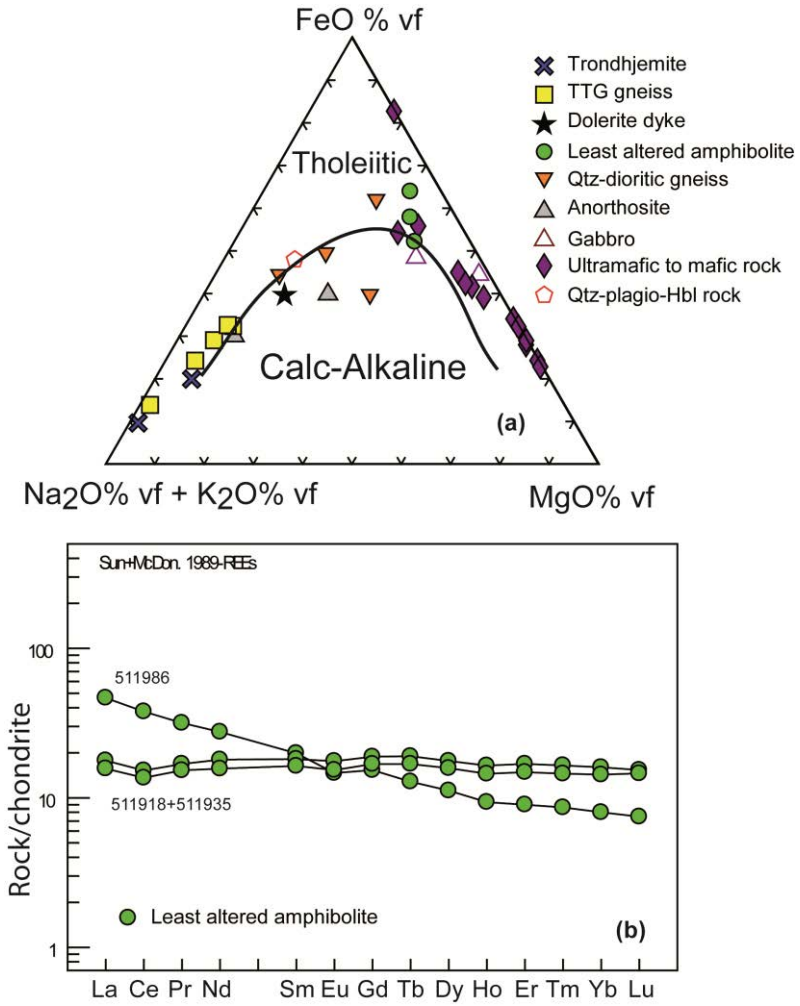

Figure 10. *Magmatic affinity **A.** Least altered samples from Bjørnesund are plotted into an AFM diagram. Most samples lie in the tholeiitic field and only a few samples are in the calc-alkaline field (vf: volatile-free basis, data were normalised after loss on ignition, LOI). **B.** Three least altered amphibolites are plotted in an REE diagram. Two samples have flat patterns indicating tholeiitic affinity and one sample shows a slightly steeper pattern indicating a tholeiitic to calc-alkaline affinity. REE data were corrected to a volatile free basis, and then normalised to the chondrite values of Sun and McDonald (1989).*

All of the ultramafic to mafic rocks and the least altered amphibolites are tholeiitic. A normalised rare earth element plot (Fig. 10B) reveals that the least altered amphibolites are tholeiitic because the patterns are flat. Sample 511986 shows a somewhat steeper pattern and it is shown later in a more detailed geochemical classification that sample 511986 represents a different chemical rock type than samples 511918 and 511935.

Rock definition of least altered and altered samples

Immobile element ratios are used to chemically classify the least altered and altered ultramafic and mafic rock samples (Fig. 11A) and to remove effects caused by hydrothermal alteration to the rocks (Barrett and MacLean, 1994, MacLean and Barrett TJ 1993).
Immobile element ratio techniques as described e.g. by Barrett and MacLean, 1994 and MacLean and Barrett TJ, 1993 allow to apply lithogeochemical methods to least altered and to altered samples.

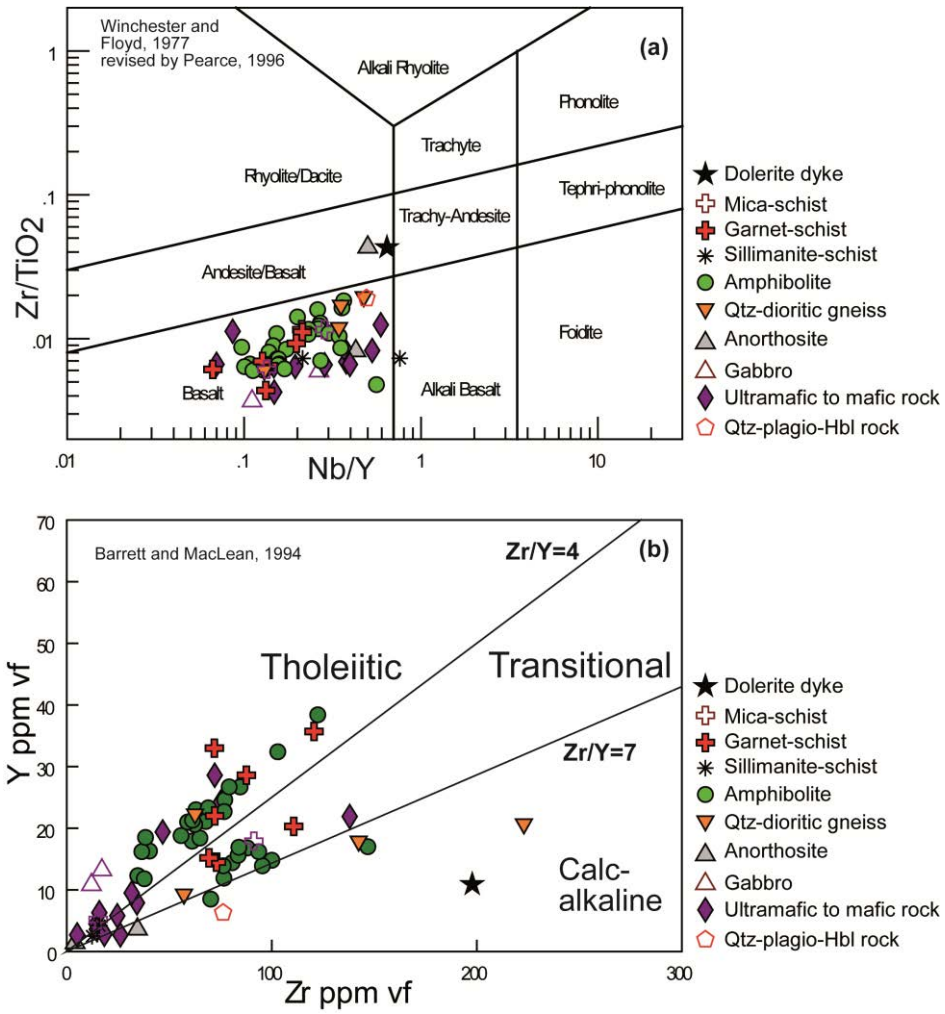

Figure 11. *Rock classification and magmatic affinity of least altered and altered samples from Bjørnesund.* ***A.*** *The Nb/Y versus Zr/TiO$_2$ diagram shows that most of the volcanic rocks and the mafic and ultramafic rocks fall into the basalt field and only a few samples are basaltic andesites.* ***B.*** *The Zr-Y diagram reveals that most of the samples are tholeiitic and transitional. Only a few samples plot in the calc-alkaline field. (Divisions from Barrett and MacLean 1994; vf = the data were normalised after loss on ignition on a volatile free basis).*

In the immobile element ratio plot of Figure 11A, all samples except one anorthosite and one dolerite dyke lie in the basalt field. The anorthosite sample and one dolerite dyke sample lie in the andesitic-basalt/basalt field. Figure 11B shows that the rocks recognized in the field as garnet-schist, sillimanite schist and mica schist fall into the same fields as the am-

phibolites and ultramafic to mafic rocks and it will be shown later that the former are hydrothermally altered amphibolites and ultramafic to mafic rocks.

Magmatic affinity of least altered and altered samples

Diagrams based on the immobile elements Zr and Y are used to assess the magmatic affinity of the least altered and altered samples (Fig. 11B). Most samples have tholeiitic affinity and few samples are of transitional and calc-alkaline affinity. The scatter plot (Fig. 11B) also shows that most ultramafic to mafic rocks have low to very low contents of Y and Zr.

Refined chemical rock definition and rock definition of least altered and altered rocks

In order to refine the rock definition of the least altered and altered rocks of the 43 amphibolite samples, we have chemically identified and accordingly classified them into the following main groups: basalt A, basalt B, basalt C, basalt D, basalt E, basalt F, basalt X (Table 1). Two samples are outliers and are in a preliminary and ad-hoc manner classified as "basalt Ti" and "amphibolite-gneiss". Future work in the area will show if these outliers are artefacts or if more samples with the same geochemical characteristics will allow to define groups for these samples.

The Zr/Y ratio was used together with the REE pattern to assess the magmatic affinity. Zr/Y ratios <4 define a tholeiitic magmatic affinity, ratios between 4 and 7 indicate a transitional (between tholeiitic and calc-alkaline) affinity, and ratios above 7 indicate a calc-alkaline affinity (See also Figure 11B; Divisions from Barrett and MacLean,1994).

Table 1. *Characteristic immobile-element ratios are used to define the Bjørnesund amphibolite and ultramafic samples into ten main chemical groups: Basalt X, basalt A, basalt B, basalt C, basalt D, basalt E, basalt F, high Mg-Cr-Ni-Co basalt, high Ti-Zr basalt and Ni-rich basalt. The chemical rock type's amphibolite-gneiss and basalt Ti belong to the chemical minor groups because only one sample falls within the amphibolite-gneiss and basalt Ti groups. The rock classification of the plutonic igneous rocks is given in Figure 8b and the criteria for these rocks are not contained in Table 1.*

Chemical main group (amphibolites and ultramafic rocks)	Statistics	Al_2O_3/TiO_2 primary rock type	Zr/Al_2O_3 primary rock type	Zr/TiO_2 primary rock type	Zr/Y rock affinity	Zr/Nb rock affinity	Nb/Y rock affinity	$Zr/10*P_2O_5$ rock affinity	La_n/Yb_n rock affinity
Basalt X	**mean**	24.2	2.7	65.1	3.1	16.7	0.2	0.1	1.2
n=2	average dev.	1.0	0.1	4.7	0.2	4.7	0.1	0.1	0.3
Basalt A	**mean**	14.4	4.4	63.2	3.0	24.8	0.1	0.6	1.0
n=11	st. deviation	1.0	0.3	2.5	0.2	3.5	0.0	0.1	0.2
Basalt B	**mean**	7.1	8.2	58.5	3.9	19.8	0.3	1.5	0.9
n=3	st. deviation	1.0	0.2	7.4	0.8	7.3	0.2	0.5	0.3
Basalt C	**mean**	11.6	6.5	74.6	4.2	16.4	0.3	0.5	3.0
n=5	st. deviation	0.9	0.6	4.3	0.9	4.2	0.2	0.4	1.5
Basalt D	**mean**	16.7	5.2	85.9	3.2	21.1	0.2	0.5	2.0
n=5	average dev.	1.8	0.4	3.7	0.7	2.3	0.0	0.2	0.5
Basalt E	**mean**	18.5	6.1	111.8	5.0	20.3	0.3	0.8	3.4
n=10	average dev.	1.5	0.4	4.7	1.0	4.2	0.0	0.2	1.1
Basalt F	**mean**	21.3	7.3	153.1	6.8	22.9	0.3	1.1	5.4
n=5	average dev.	3.6	0.7	15.4	1.4	2.4	0.1	0.7	3.9
High Mg-Cr-Ni-Co basalt	**mean**	16.4	5.5	77.8	5.2	15.1	0.4	0.0	2.9
n=5	average dev.	6.1	2.1	18.6	2.3	6.1	0.1	0.0	1.3
High Ti-Zr basalt	**mean**	13.7	5.4	71.5	3.6	21.9	0.2	0.8	1.4
n=4	average dev.	1.4	1.1	5.9	1.4	7.6	0.2	0.4	0.9
Ni-rich basalt	**mean**	69.1	3.1	76.9	3.5	23.6	0.2	0.1	2.0
n=4	average dev.	58.8	2.1	23.1	0.9	12.2	0.1	0.1	1.2
Chemical minor group									
amphibolite-gneiss	n=1	21.7	9.8	212.2	10.4	21.2	0.5	3.34	9.91
Basalt Ti	n=1	7.8	5.6	43.5	3.1	23.2	0.1	0.62	0.90

The refined chemical rock classification is based on the immobile element ratios Al_2O_3/TiO_2, Zr/Al_2O_3, Zr/TiO_2 and each chemical rock type has its characteristic range of the Al_2O_3/TiO_2, Zr/Al_2O_3, Zr/TiO_2 Ratios. The average deviation of the samples is given for each chemical group and reveals that sample spread within a given chemical group is relatively small (table 1). This is best shown graphically on the scatter plots Zr/TiO_2 vs. Zr/Al_2O_3 (Fig. 12A), Al_2O_3/TiO_2 vs. Zr/Al_2O_3 (Fig. 12B) and Al_2O_3/TiO_2 vs. Zr/TiO_2 (Fig. 12C).

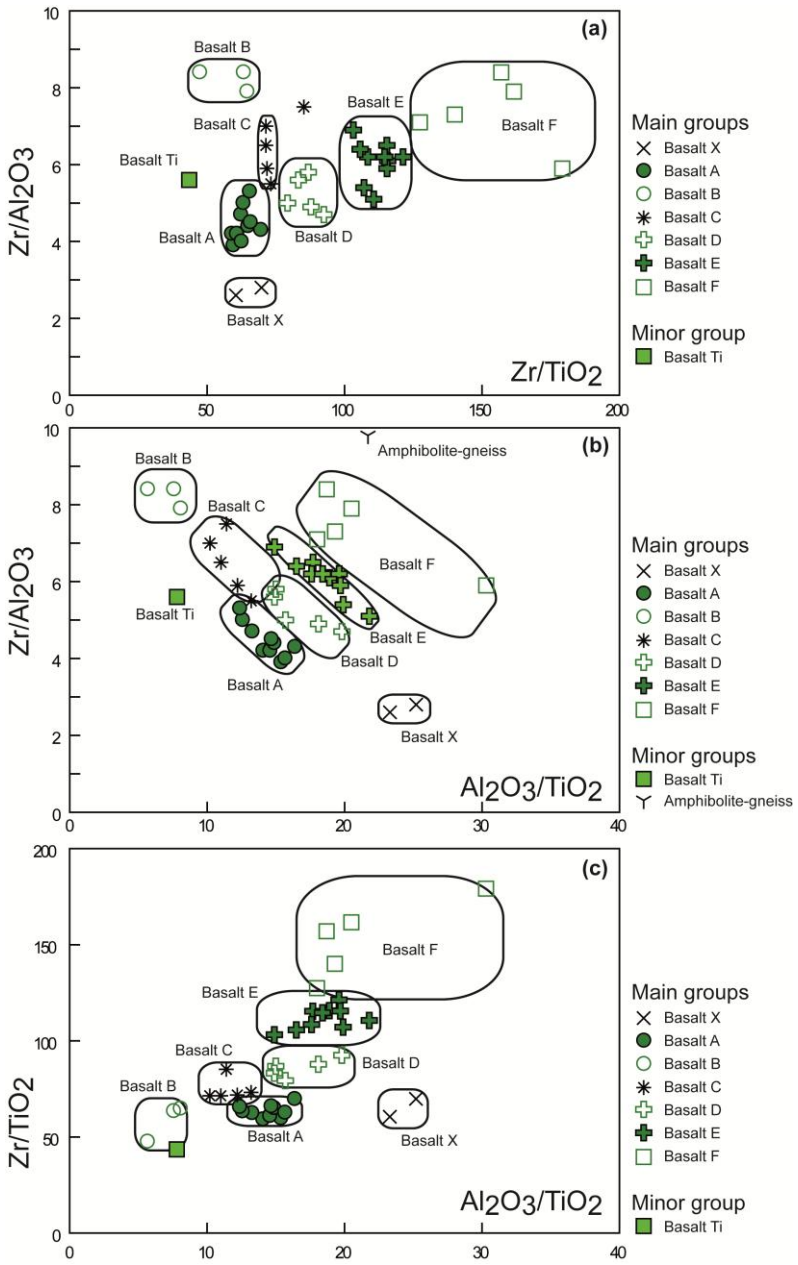

Figure 12. *Refined rock classification based on immobile element ratio plots.* ***A.*** *Zr/TiO_2 versus Zr/Al_2O_3 diagram.* ***B.*** *Al_2O_3/TiO_2 versus Zr/Al_2O_3 diagram.* ***C.*** *Al_2O_3/TiO_2 versus Zr/TiO_2 diagram. Figure 12.C shows that the amphibolites from Bjørnesund can be classified into seven main groups and two minor groups based on immobile element ratios. The main chemical rock types are basalt X, basalt A, basalt B, basalt C, basalt D, basalt E and basalt F. The minor chemical rock types are basalt Ti and amphibolite-gneiss (Divisions from Barrett and MacLean 1994).*

Scatter plots (Figs. 12A to 12C) show that the chemical groups fall into relatively well defined fields. The ternary plot of Figure 13A shows that the seven main chemical groups are clustered in this diagram and fraction trends are tentatively indicated in Figure 13B. It is necessary to sample and analyse additional least-altered amphibolites from each of the seven chemical main groups in order to verify if different magmatic fractionation trends occur.

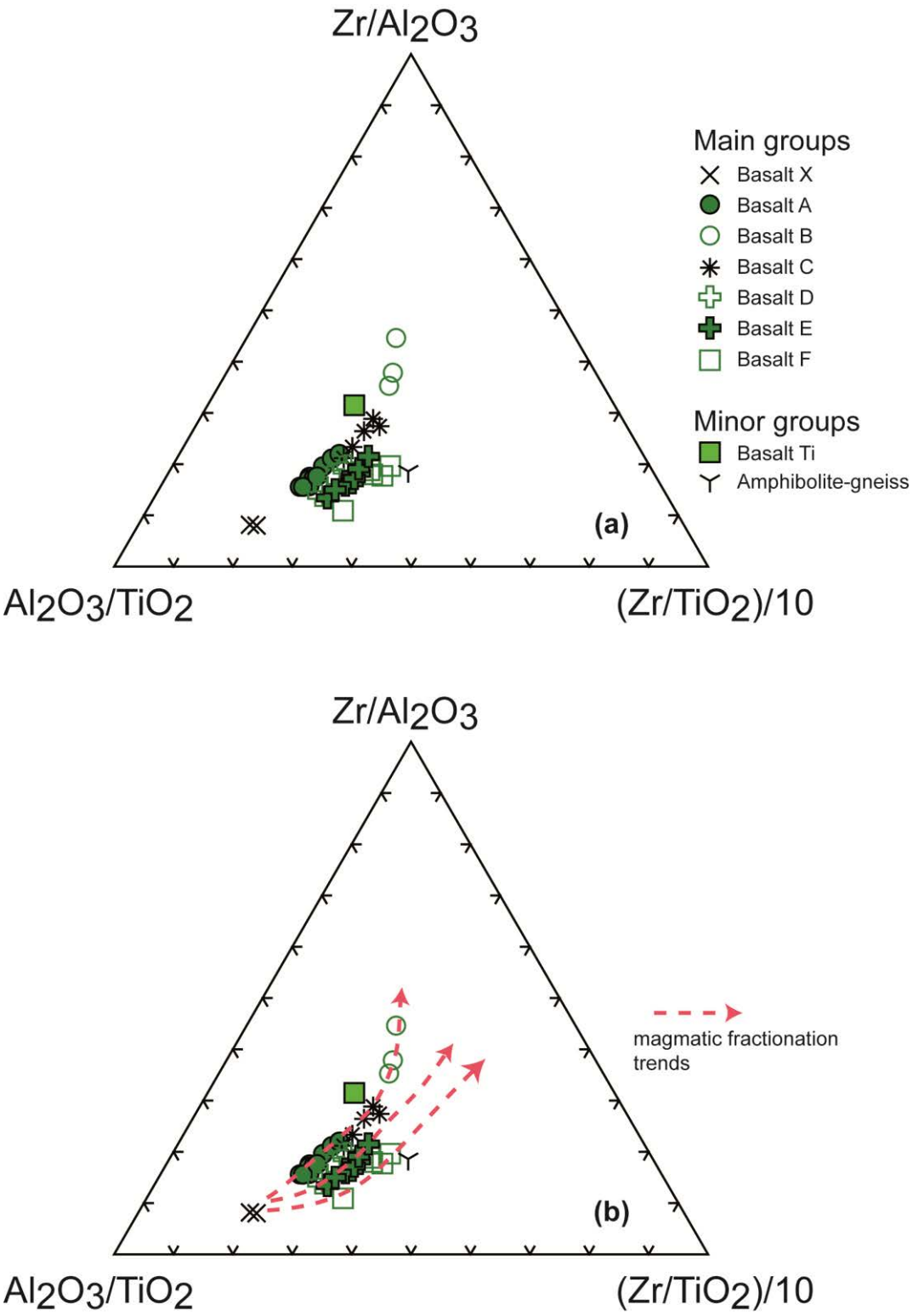

Figure 13. ***A.*** *A ternary plot based on the ratios Zr/Al_2O_3, Al_2O_3/TiO_2 and $(Zr/TiO_2)/10$ reveals that the 7 main chemical rock groups form fairly tight clusters.* ***B.*** *On the same plot as shown in A. trends are superimposed which could correspond to three different magmatic fractionation trends.*

Geochemical characteristics of primary rocks of the sub-areas Bjørnesund West, Bjørnesund East and Bjørnesund further East

The primary geochemical characteristics of the amphibolites occurring in the Bjørnesund West (Fig. 14A) and Bjørnesund East areas (Fig. 14B) are very similar. Seven main groups can be distinguished based on the variation of immobile-element ratios: basalt X, basalt A, basalt B, basalt C, basalt D, basalt E and basalt F (Table 1). These seven main groups of amphibolites are found in the Bjørnesund West as well as in the Bjørnesund East area (Figs 14A and b).

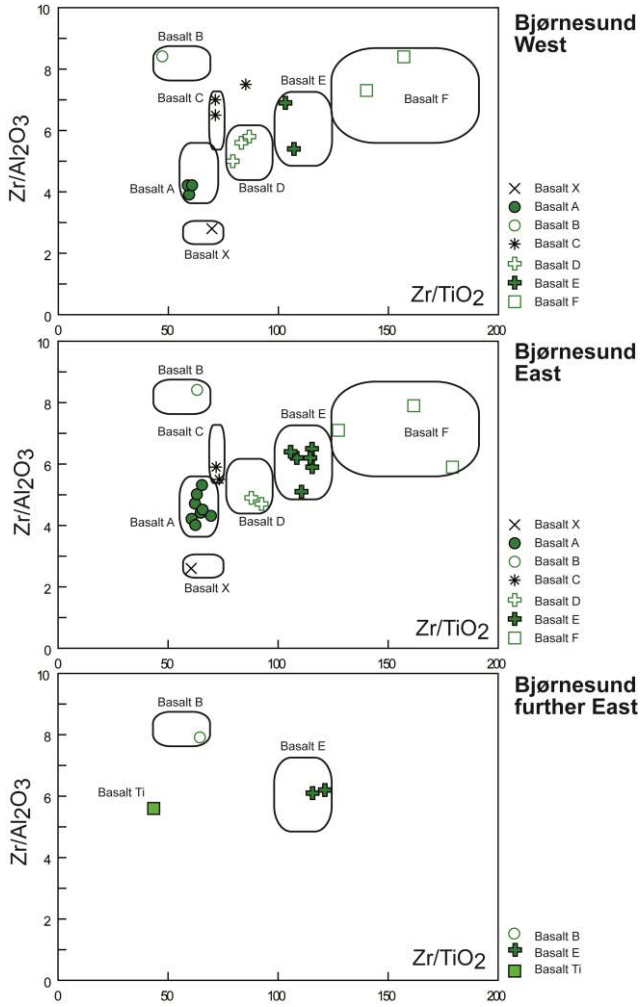

Figure 14. *Primary composition and distribution of rock types in the three Bjørnesund subareas.* ***A.*** *In the Bjørnesund West area all the main chemical groups occur: basalt X, basalt A, basalt B, basalt C, basalt D, basalt E and basalt F.* ***B.*** *In the Bjørnesund East area all the chemical main groups occur: basalt X, basalt A, basalt B, basalt C, basalt D, basalt E and basalt.* ***C.*** *In the Bjørnesund further East area only the chemical main groups basalt B and basalt E occur, and one sample of basalt Ti sample from the minor chemical group also occurs. The reason that only a few rock types were encountered could be related to the sparse sampling in this area.*

This geochemical assessment supports the teconic model suggested by Keulen *et al.* (2010a) postulating that the Bjørnesund West and Bjørnesund East areas belong to the

same Bjørnesund Anorthosite-Greenstone belt. In the Bjørnesund area further to the East only four amphibolites were sampled: basalt B, basalt E and basalt Ti. Interestingly, basalt Ti was not encountered in the Bjørnesund subareas further towards the west. The amphibolites in all sub-areas of the Bjørnesund Anorthosite-Greenstone belt have very similar geochemical characteristics and likely were interconnected prior to post-emplacement tectonic dismemberment.

Primary composition and position of tectonostratigraphic units of the Bjørnesund West area

Sampling and chemical identification of the Bjørnesund West area (Table 1, Fig. 15) reveals that the amphibolites (plotted in green colour) are all of basaltic composition. In the Bjørnesund West area all main chemical groups are found and the most abundant groups are basalt A, basalt C and basalt D. The amphibolite sample which yields 569 ppb gold falls in the basalt E group (Fig. 15).

A preliminary chemostratigrapic assessment reveals that basalt E rocks are intercalated between a package of basalt A immediately towards the NW and a package of basalt C towards the SE.

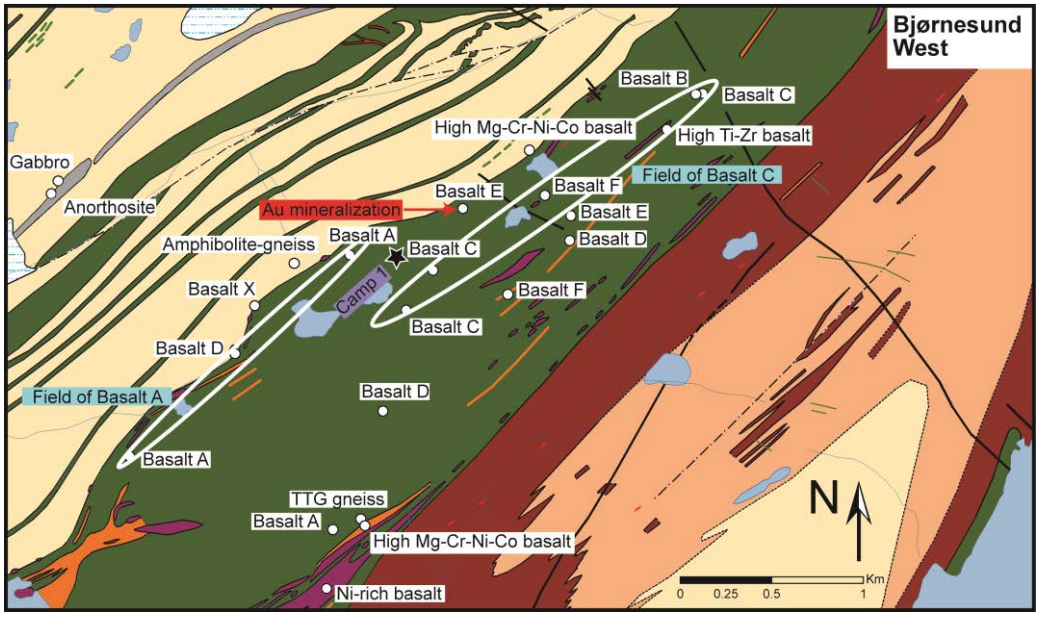

Figure 15. *Chemostratigraphic relation seen from the Bjørnesund West area. A rock unit which comprises mainly basalt A and a unit comprising mainly basalt C can be identified based on lithogeochemical techniques. The gold mineralisation is hosted in rocks of basalt E type, and have basalt A in the structural footwall and basalt C in the structural footwall. For legend see Figure 4.*

Geochemical studies also confirm the occurrence of ultramafic rocks in the Bjørnesund West area. In details these rocks were identified as high Mg-Cr-Ni-Co basalt, high Ti-Zr basalt and Ni-rich basalt and are located in the northern and in the southern parts of the

Bjørnesund West are (Fig. 15). Geochemical studies also confirm that the small sequence of anorthosites that crops out in the western part of the Bjørnesund West area (Fig. 15) comprises anorthositic and gabbroic rocks.

Primary composition and position of tectonostratigraphic units of the Bjørnesund East area

The amphibolites of the Bjørnesund East area (see the areas of Figure 16 plotted in green colour) are of basaltic composition and basalt A and basalt E are the most abundant groups (Table 1, Fig. 16).

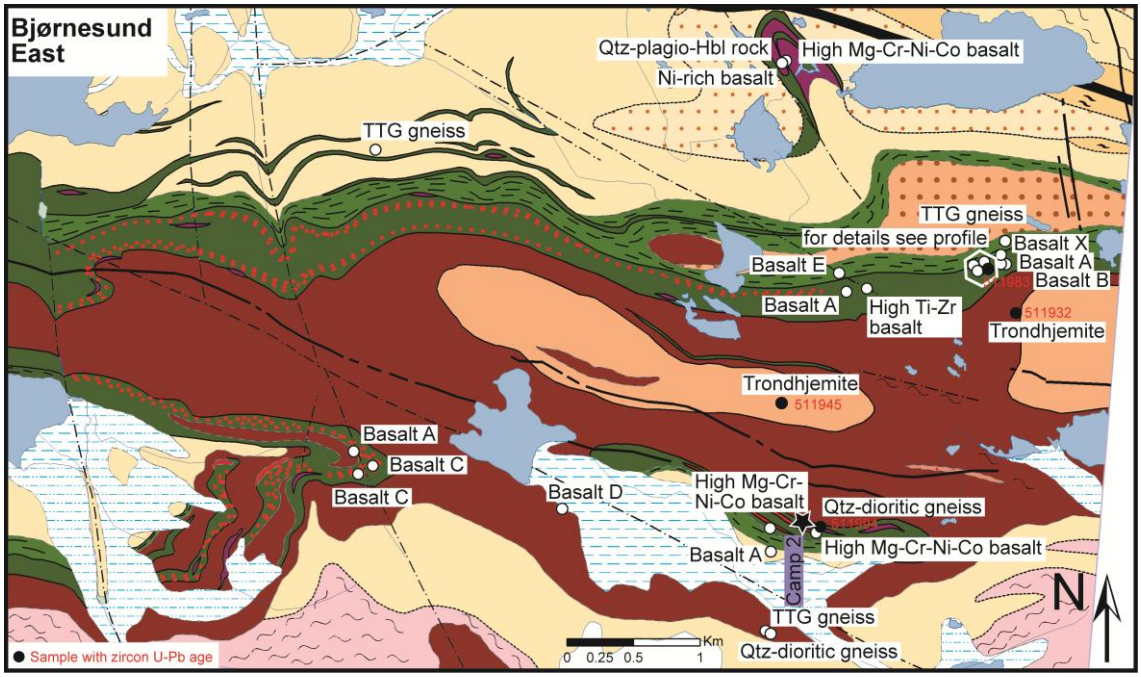

Figure 16. *Chemostratigraphic relation seen from the Bjørnesund East area. Basalt A rocks occur on the northern and on the southern limb of the Bjørnesund East area and are in agreement with the structural model presented by Keulen et al. (2010). In general there is good agreement between geological mapping of the rock units and chemical primary rock types. In several cases geochemistry has helped to improve the mapping(e.g., the unit mapped as granite is a trondhjemite as seen from the geochemical classification;see Figure 8). Details of the chemostratigraphic relation of the tectonostratigraphic sequence (profile Bjørnesund East) area are given in Figure 17. For legend see Figure 4.*

The granitic body in the centre of the Bjørnesund East area (Fig. 16) is of trondhjemititc composition. The large areas mapped in brown are diorites and are of Qtz-dioritic composition. Gneisses which have intruded the anorthosite-grenstone belt are of TTG composition. Geochemical work has also confirmed the occurrence of ultramafic rocks in the Bjørnesund East area (Fig. 16). These rocks were identified as high Mg-Cr-Ni-Co basalt, high Ti-Zr basalt and Ni-rich basalt and are located as an exotic ecaille (imbricate structure) within the TGG gneisses in the northern part of the Bjørnesund East area (Fig. 16).

Chemostratigraphic investigation of the detailed profile

The detailed tectonostratigraphic sequence of Bjørnesund East has been shown earlier (Fig. 5). Here we demonstrate how the detailed sampling of 13 rock samples across this surface profile has allowed the establishment of the chemostratigpraphy. For each of the 13 samples of the tectonostratigraphic sequence the primary rock type was determined by applying the criteria defined by different ranges of immobile element ratios characteristic for each chemical group (Table 1). Figure 17 shows the variation in primary rock types of the Bjørnesund East profile.

The structural FW comprises massive Qtz-dioritic gneiss, and the Bjørnesund East ore horizon comprises basalt A and basalt E. The structural HW is made up of a thick sequence of basalt A and a thick sequence of basalt E and basalt F. A relatively thin unit of basalt D occurs between these two sequences. It is conceivable that these changes in primary rock type correspond to different basaltic flows deposited on the sea-floor which is in agreement with descriptions of distinct pillow textures observed in the Bjørnesund area by Pulvertaft (1972). Each of these units is a few meters thick and the locus of the gold mineralization occurs at the contact of basalt A and basalt E. Interestingly, the locus of the gold mineralization at Bjørnesund West and the sample with 569 ppb gold are also located at a contact between basalt A and basalt E.

Characterization of hydrothermal alteration and mineralization

It has been shown in an earlier section that the hydrothermal alteration minerals of the Au-zones in Bjørenesund West and Bjørenesund East are predominately quartz, biotite, muscovite, sulphide and oxyhydroxides. In both areas hydrothermal alteration is related to shear zones.

Alteration in the outcrops in the Bjørnesund West area where new gold mineralization was found (Figs. 15 and 18A) was investigated using the sample that yielded 569 ppb gold.

Electron probe microanalysis reveals that hornblende and garnet are intimately affected by minuscule stockwork-like stringers of iron oxide-hydroxide (Fig. 18B). Other areas of the examined thin section comprise patches of iron oxide-hydroxide (Fig. 18B). Other hydrothermal alteration zones comprise centimetre-thick quartz-carbonate-plagioclase veinlets. These veinlets also contain chlorite, apatite, mica and iron oxide-hydroxides.

Future geological field work and sampling is necessary to better characterize this newly discovered gold zone of the Bjørnesund West area and to assess the economic potential.

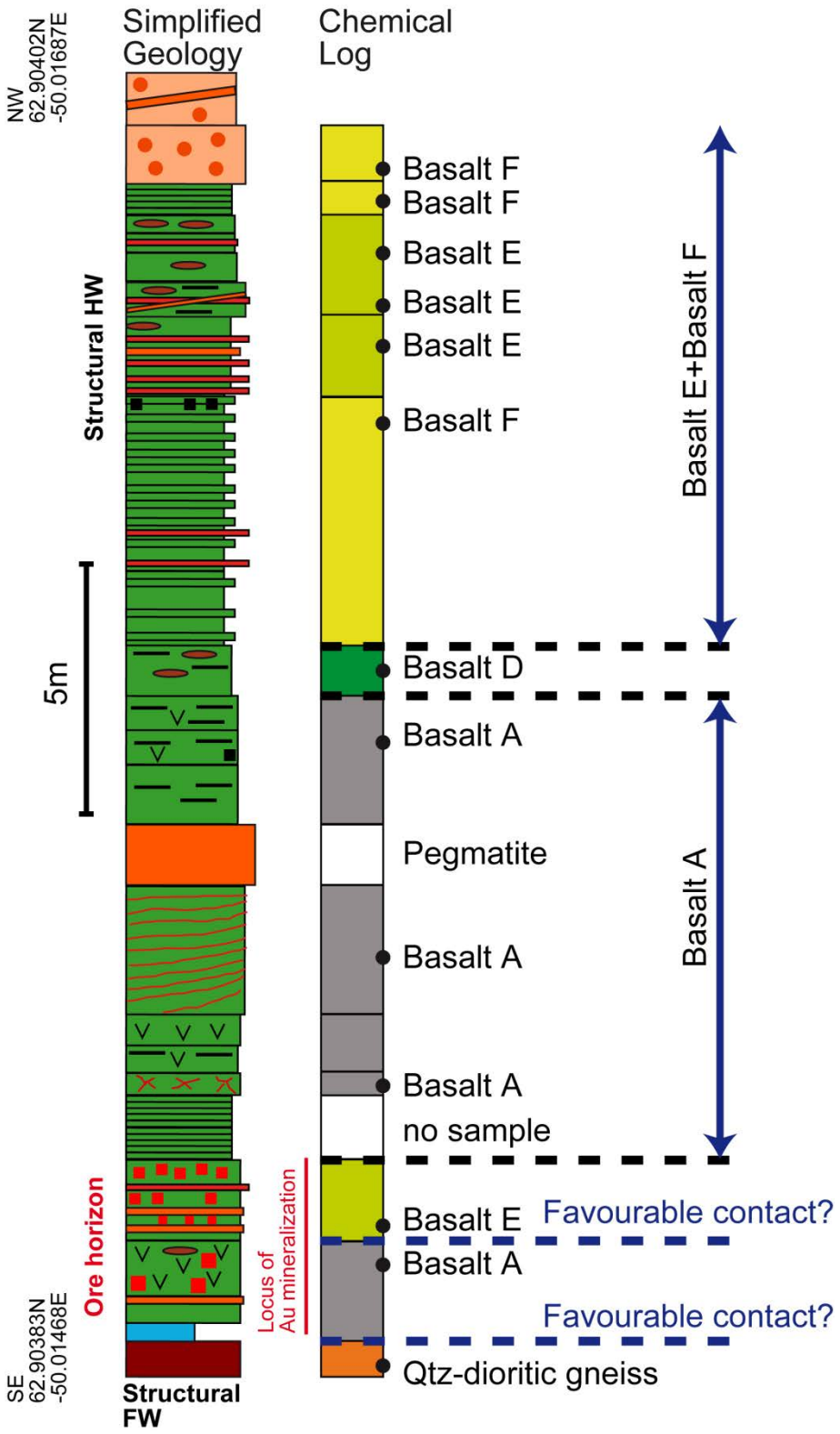

Figure 17. *Chemostratigraphic relations seen from the tectonostratigraphic sequence located in the eastern part of Bjørnesund East. The locus of the gold mineralisation is between Qtz-dioritic gneiss and a sequence of rocks comprising predominately basalt A together with lesser basalt E and D. The structural hanging wall comprises basalt F and basalt E. A pegmatite that has intruded the tectonostratigraphic sequence was not sampled. For legend see Figure 5.*

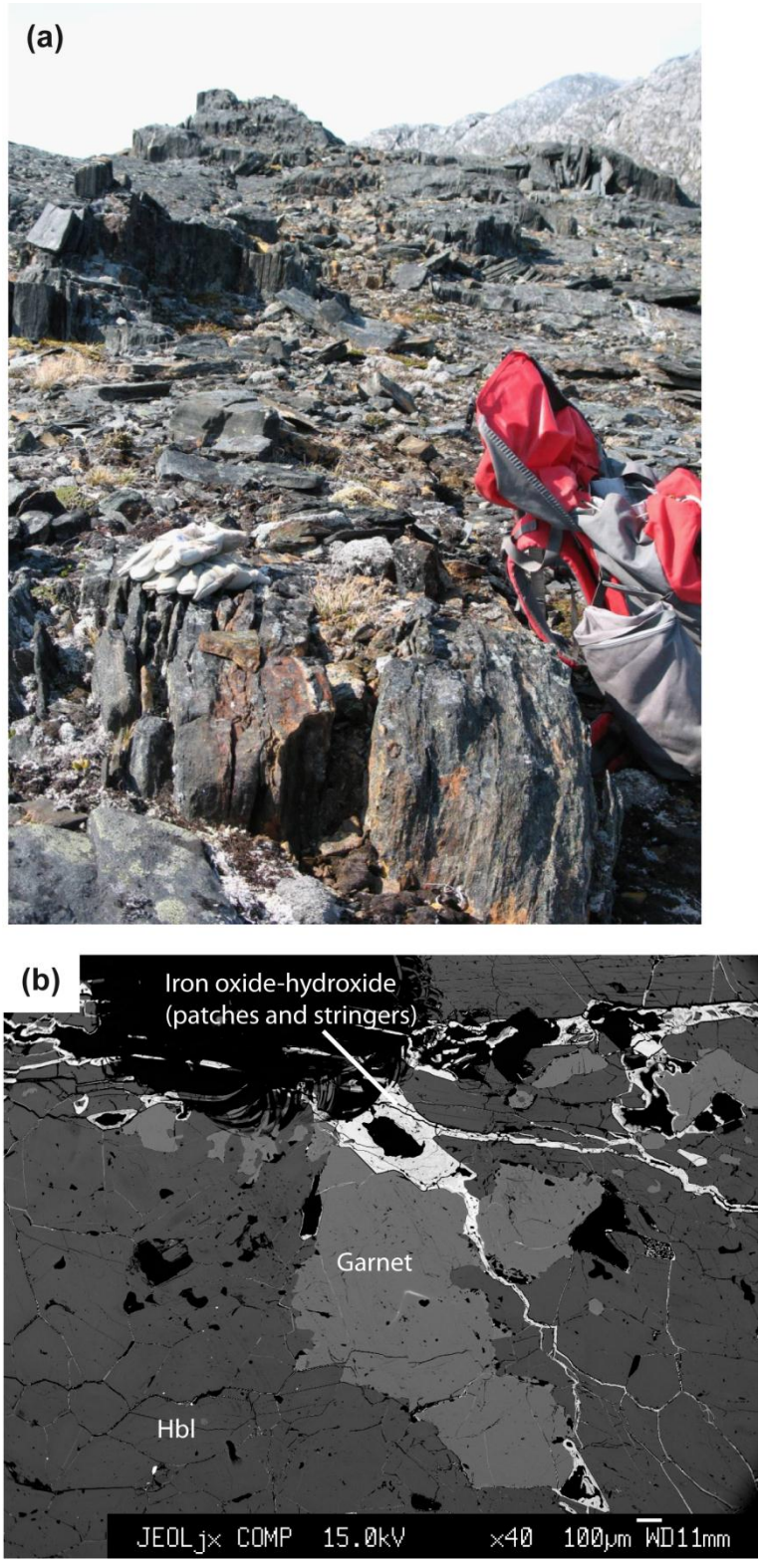

Figure 18. *New gold occurrence at Bjørnesund West **A.** Photograph of sheared rusty amphibolite containing 569 ppb gold. The structure can be followed for several hundred meters along strike. **B.** BSE image from the garnet and iron oxide-hydroxide altered amphibolite with 569 ppb gold from the new gold occurrence at Bjørnesund West. Sample shown in B. is 511907-B.*

Alteration as assessed from TiO_2 versus Zr plots

On a TiO_2 versus Zr diagram, rocks belonging to the same chemical group form alteration trends (MacLean and Barrett 1993). It has been shown earlier that the immobile element ratios can be used to group the Bjørnesund samples into 18 primary rock types (Table 1). Hydrothermal alteration has resulted in the loss of the mobile elements, leading to a residual concentration of the immobile elements. These effects do not change the initial ratio between two immobile elements for a given chemical rock type.

Some rock types as seen from Figures 19A and 19B such as the high Mg-Cr-Ni-Co basalts are only moderately altered as indicated by the clustered Zr vs. TiO2 data and lack of an alteration trend. Basalt C from the Bjørnesund West area and Basalt A and basalt E from the Bjørnesund East area form distinct alteration trends and are therefore hydrothermally altered (Figs. 19A and 19B). Too few samples from the Bjørnesund further East area are available to assess if this area was affected by hydrothermal alteration.

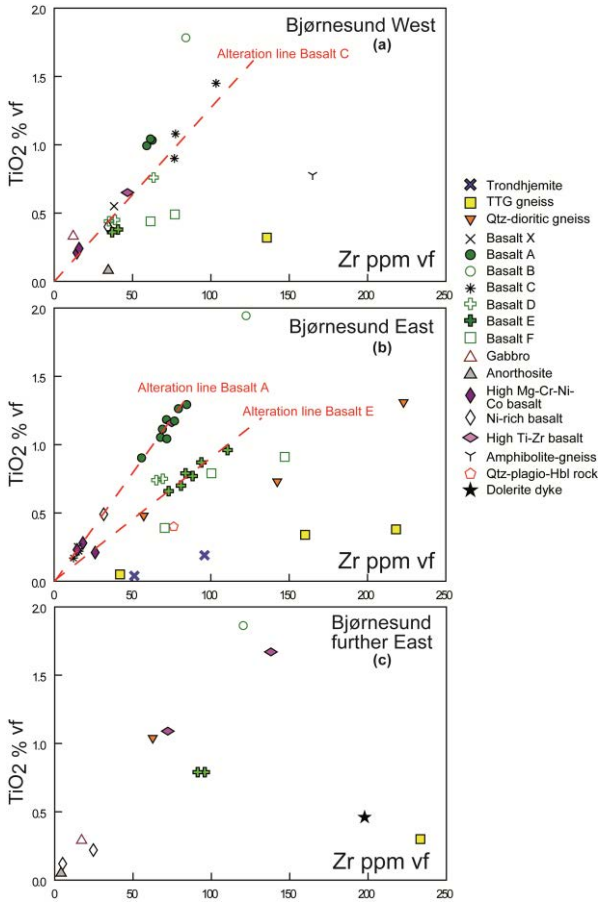

Figure 19. *A Zr versus TiO_2 plot is used to estimate the intensity of the hydrothermal alteration. Altered samples define elongated fields.* ***A.*** *Only the amphibolite samples from Bjørnesund West define an alteration trend, which is best seen from basalt C samples. The other rock types are less altered or least altered.* ***B.*** *Bjørnesund East samples are altered similarly to samples from Bjørnesund West. In the Bjørnesund East area the basalts A and basalts E define alteration trends.* ***C.*** *Samples from Bjørnesund further East do not plot on alteration trends; this area was sampled in much less detail than the Bjørnesund West and the Bjørnesund East areas. (vf: volatile free basis).*

Correlation between Au and pathfinders of rock samples

It is suggested that the same hydrothermal fluids that caused alteration are also responsible for the introduction of gold to the host rock.

The elements enriched in the host rock together with gold during the mineralization process are of particular interested because they can cause alteration halos larger than the extent of the gold mineralization. Recognizing such alteration halos and pathfinder elements in the field is important as these might indicate a nearby gold mineralization.

In order to assess which elements are fluid-transported together with gold, As, Bi, W, Sb, Cu, Zn, Sc and Cs were plotted versus the gold on a scatter diagram (Fig. 20). The scatter diagrams reveal that none of these elements show a strong correlation with gold, however one sample with high Bi content and elevated gold occurs in the Bjørnesund further East area (Fig. 20B).

It is interesting that the sample with the highest gold has low As, Bi, W, Cu, Sc and Cs contents, but is elevated in Sb and Zn (Fig. 20). Hence Sb and Zn seem to be the most interesting element to identify a proximal alteration zone in the Bjørnesund areas (Fig 20D and 20F).It is known from other gold mineralisations that certain elements such as arsenic can indicate a medial to distal part of the alteration system related to the gold mineralising event (Schlatter and Kolb 2011). Arsenic can still be used in these cases as a useful pathfinder in combination with a second set of pathfinders such as Sb or Bi.

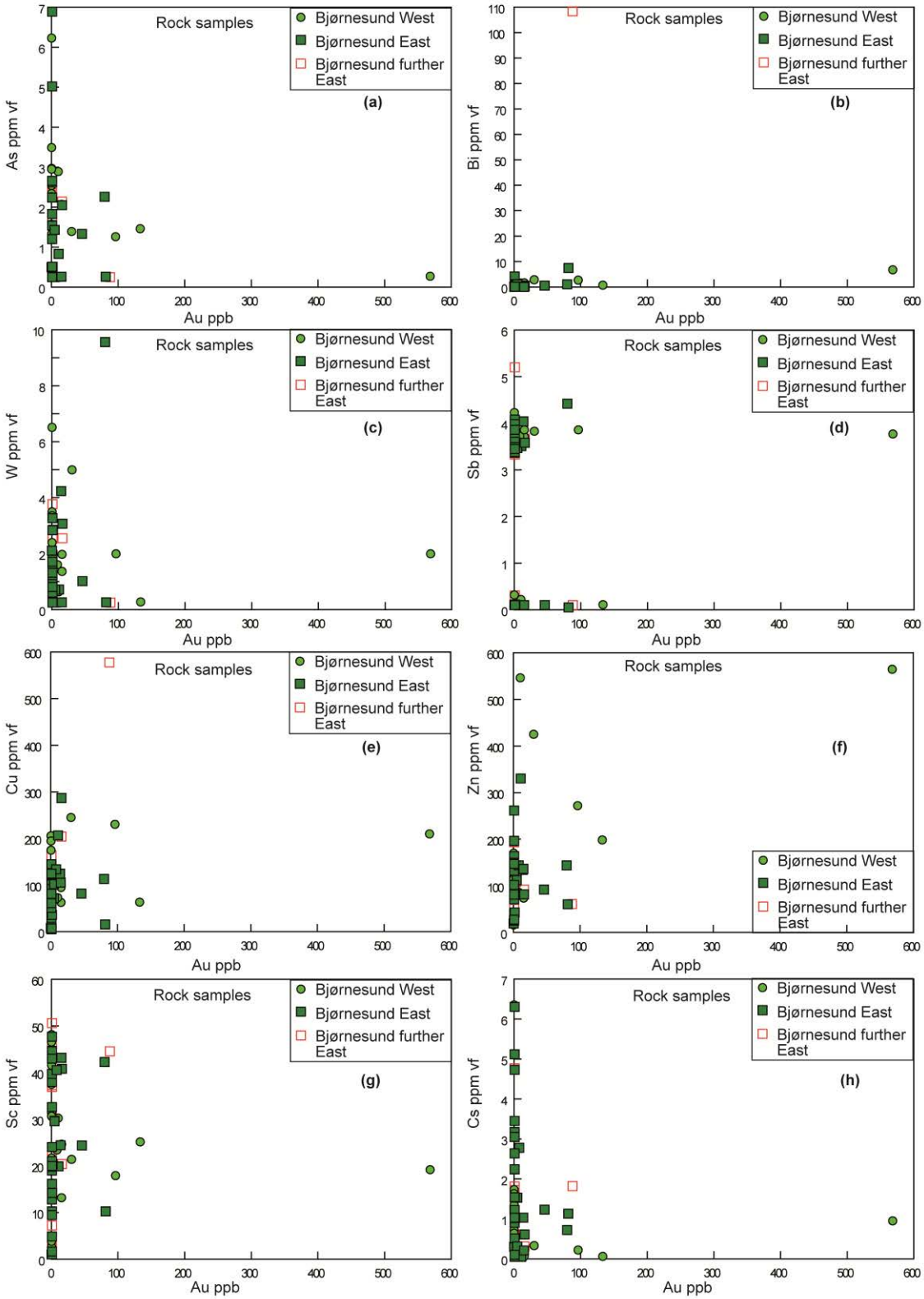

Figure 20. *Gold and metal distribution of rock samples.* ***A.*** *Scatter plot of Au versus As.* ***B.*** *Scatter plot of Au versus Bi.* ***C.*** *Scatter plot of Au versus W.* ***D.*** *Scatter plot of Au versus Sb.* ***E.*** *Scatter plot of Au versus Cu.* ***F.*** *Scatter plot of Au versus Zn.* ***G.*** *Scatter plot of Au versus Sc.* ***H.*** *Scatter plot of Au versus Cs.*

Correlation between Au and pathfinders of sediment samples

Thirty-nine new sediment samples were collected in the Bjørnesund area and tested for correlation between Au and the pathfinders which were identified from the rock samples (Fig. 21). Some correlation between Au and Zn (Fig. 21D) might exist. The Au-Sb plot (Fig. 21B) is highly scattered. Au and As are weakly correlated (Fig. 20A) and several sediment samples have high arsenic contents (Fig. 20A). The two sediment samples that are elevated in Au have also elevated As contents possibly indicating a medial to distal alteration zone.

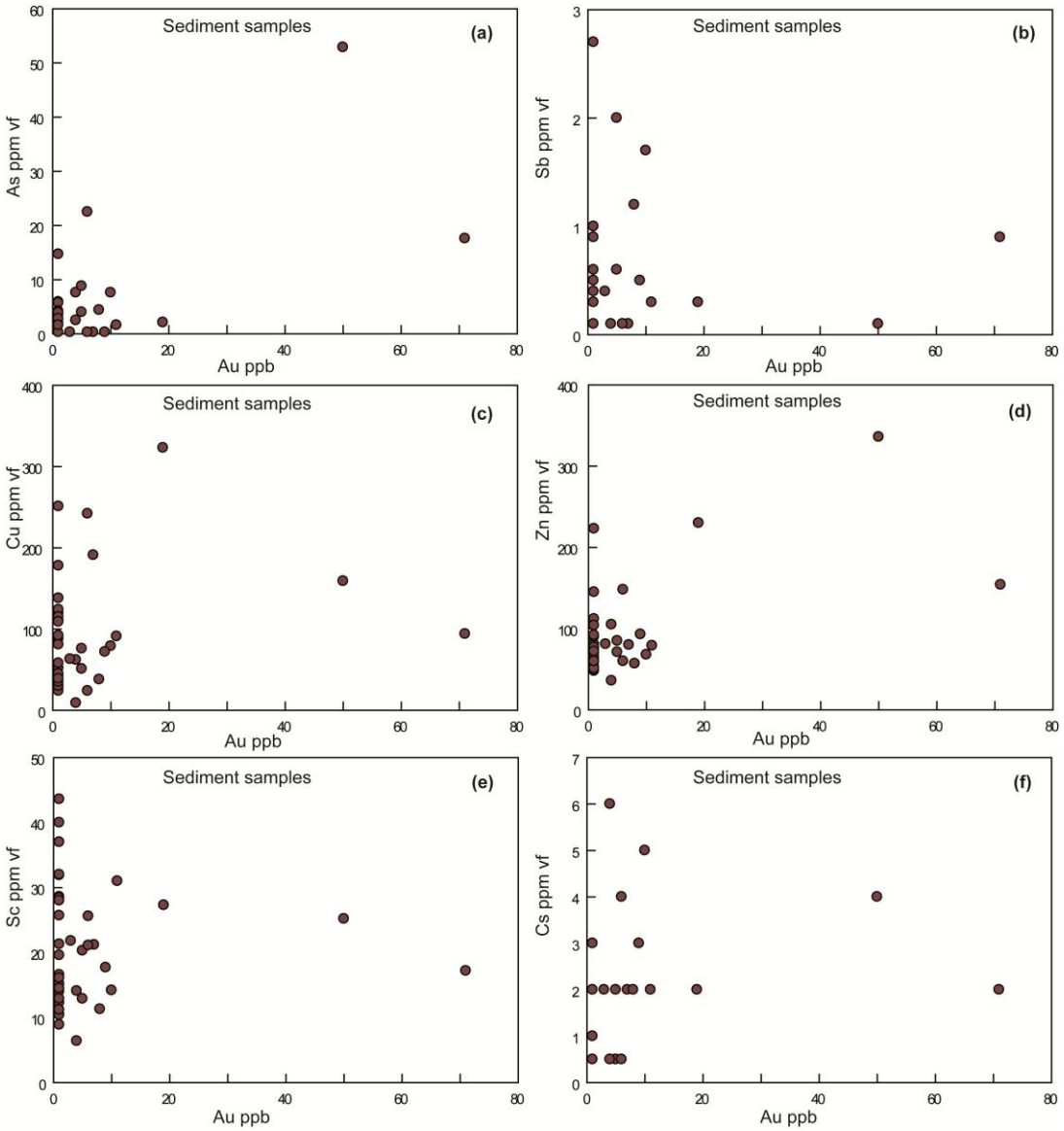

Figure 21. *Gold and metal distribution of sediment samples.* ***A.*** *Scatter plot of Au versus As.* ***B.*** *Scatter plot of Au versus Sb.* ***C.*** *Scatter plot of Au versus Cu.* ***D.*** *Scatter plot of Au versus Zn.* ***E.*** *Scatter plot of Au versus Sc.* ***F.*** *Scatter plot of Au versus Cs.*

Gold anomalous rock samples of the Bjørnesund East and West areas

Only three rock samples have gold contents above 100 ppb and these samples were collected in the Bjørnesund West area (Fig. 22).

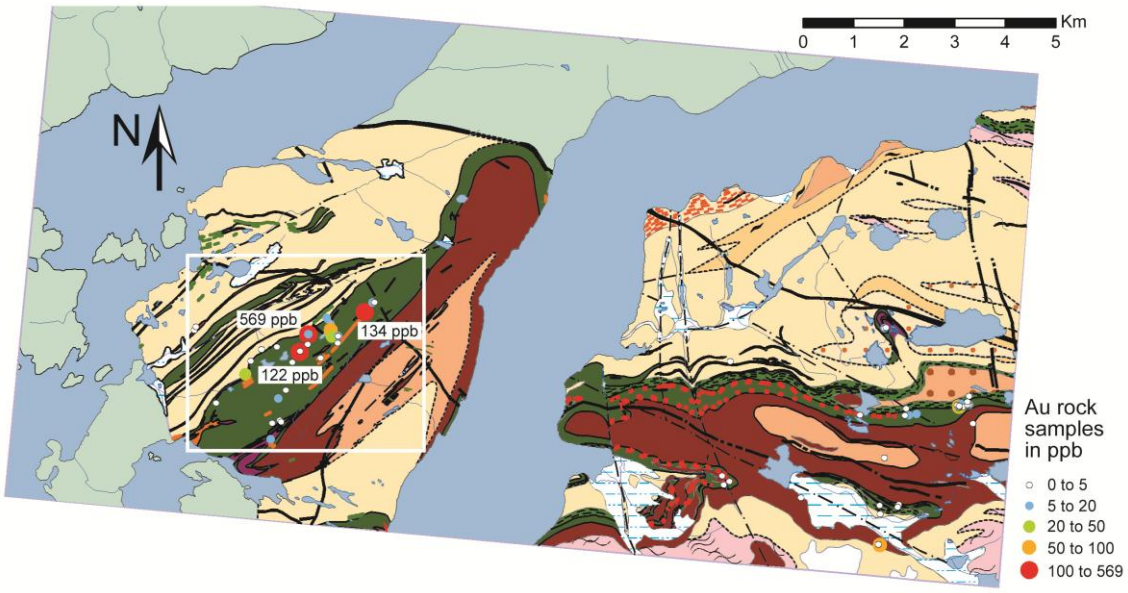

Figure 22. *Gold anomaly plot of rock samples of the Bjørnesund West and the Bjørnesund East areas. The highest gold anomalies from rock samples stem from the Bjørnesund West area whereas in the Bjørnesund East area only a few rock samples yield gold above 50 ppb. (In Figure 22 a small box provides the outline of an area that is discussed in more details in Figure 24). For legend see Figure 4.*

These samples are located in a potentially gold mineralized NE-SW trending corridor of at least 1500 m. This gold mineralized corridor possibly continues towards the SW as indicated by one rock sample with anomalously elevated gold of 31 ppb located 1100 m to the south-west of the sample with 122 ppb gold (Fig. 22).

Gold anomalous sediment samples of the Bjørnesund East and West areas

Only two sediment samples have gold contents that are equal or above 100 ppb and these samples are located in the Bjørnesund east area (Fig. 23). Both samples are located in the same NE-SW trending corridor which was described from the anomalous rock samples.

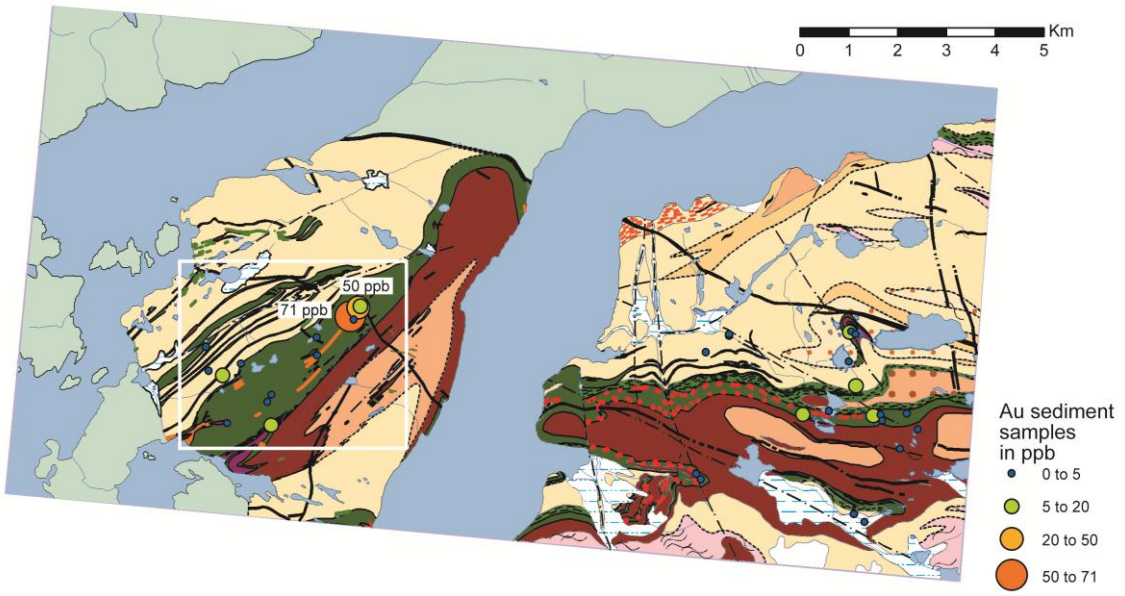

Figure 23. *Gold anomaly plot of sediment samples in the Bjørnesund West and the Bjørnesund East areas. The highest gold anomalies from rock samples stem from the Bjørnesund West area whereas in the Bjørnesund East area only a few rock samples yield gold above 5 ppb. (In Figure 22 a small box provides the outline of an area that is discussed in more details in Figure 24). For legend see Figure 4.*

Discussion

New anomalously high gold values were found in the Bjørnesund West area (Fig. 24) and the potential of this area is supported by anomalous Au contents of rock and stream/scree sediment samples. This area is relatively sparsely sampled (Fig. 24) and only future gold exploration will show how many of the hydrothermally altered shear zones are gold mineralized and if the area hosts gold in economic grades and quantities. In contrast, the Bjørnesund East area (Fig. 25) is more densely sampled; however, gold contents are rarely above 100 ppb and never higher than 200ppb.

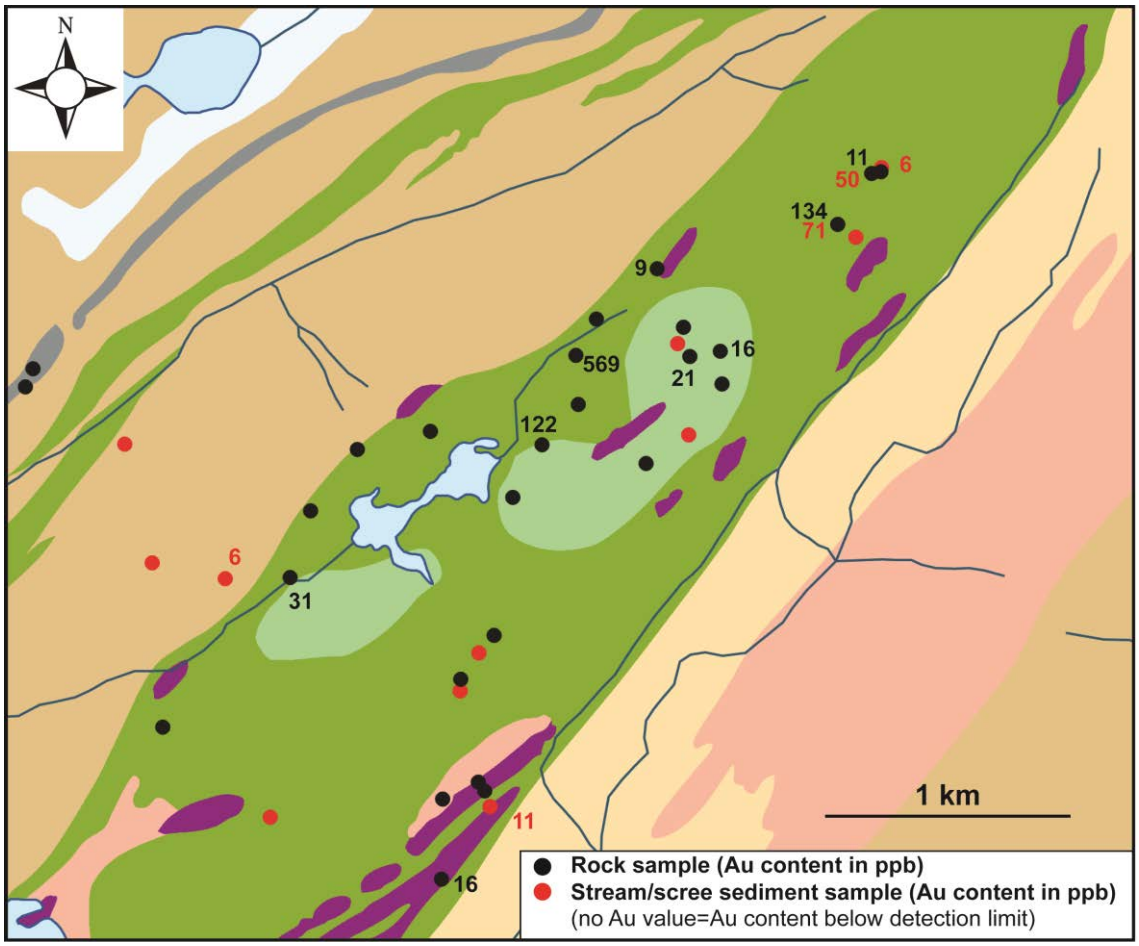

Figure 24. *Gold anomaly plot of sediment samples from sediment samples in the Bjørnesund West area. A several tens-of-metres wide shear zone was studied at 50°16.2'W and 62°54.4'N at 555 m elevation above sea level in the Bjørnesund West area. It can be followed over several hundred-of-metres along strike and rock samples yield 122, 569 and 134 ppb gold. This shear zone contains a 50 cm yellow-brownish, rusty stained amphibolite, which hosts parallel quartz-carbonate veinlets. Chip samples over 50 cm yielded 569 ppb Au, whereas a similar amphibolite 1.5 km towards southwest yielded 31 ppb over about 10 m. This same zone which returned several rock samples with strongly anomalously elevated gold contents has also returned sediment samples that are elevated in gold. For legend see map sheet Bjørnesund 62V.1 NORD, 1:100 000.*

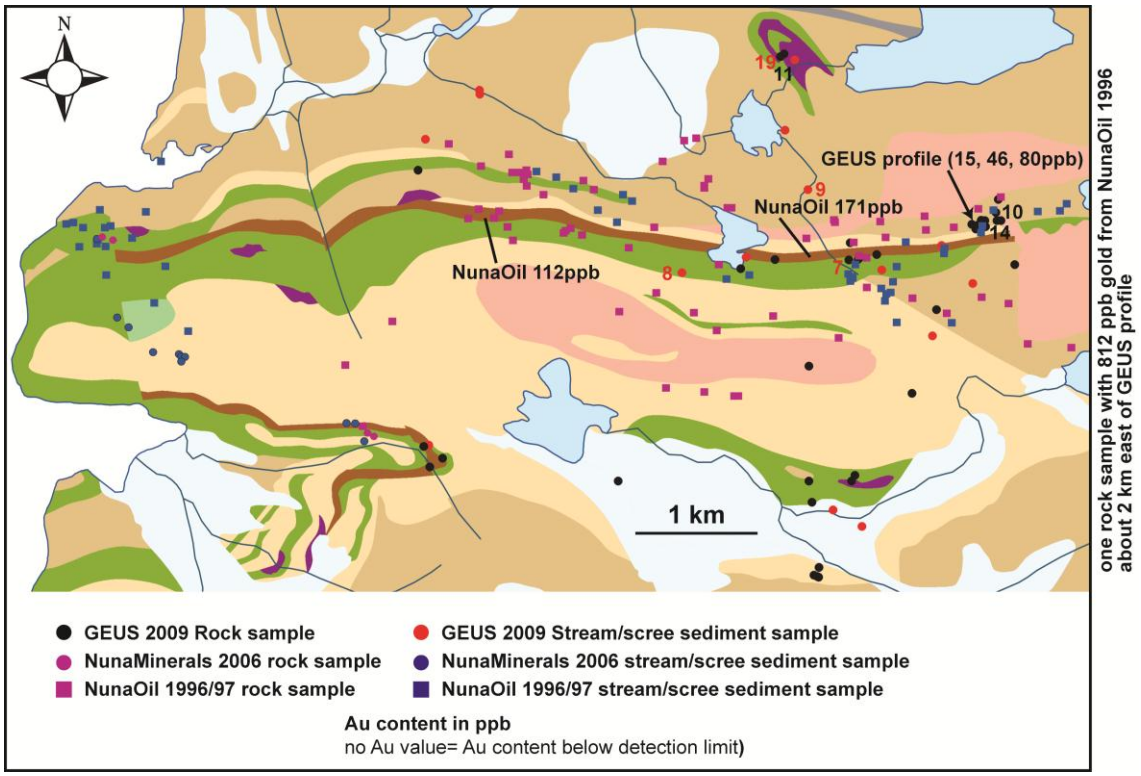

Figure 25. *Gold distribution as seen from rock and sediment samples in the Bjørnesund East area. Several rocks with elevated gold with contents of above than hundred ppb have been reported from earlier work by NunaOil A/S in the 1990's. These zones with elevated gold are located in a thrust-shear zone located between meta-quartz-diorite and gneiss and this structure can be followed for at least 10 km along strike. For legend see map sheet Bjørnesund 62V.1 NORD, 1:100 000.*

It is possible that the Bjørnesund East area corresponds to a frontal ramp where lesser gold is to be expected because of a compressive regime. On the other hand the Bjørnesund West area corresponds to a lateral ramp where associated shear zones represent good traps for gold mineralisation.

The spatial association of gold mineralized rocks and the granite trondhjemite rocks in the Bjørnesund West and the Bjørnesund East areas is intriguing. However, timing of the gold mineralization is unknown and it is not possible to determine if the emplacement of the granite trondhjemite rocks and the gold mineralization is contemporaneous. The genetic associations between gold mineralization and felsic plutonic intrusions were documented from areas where more geological data are available (Groves *et al.* 2003, Eilu and Groves 2001).

Conclusion and recommendations for future work

This new occurrence at Bjørnesund West can be put into the regional context because several rocks with elevated gold of several hundred ppb have been reported from earlier work done by NunaOil A/S in the 1990s in the region east of Bjørnesund. These zones with elevated gold are located in a thrust-shear zone located between meta-quartz-diorite and gneiss and this structure can be followed for at least 10 km along strike (Fig. 26A).

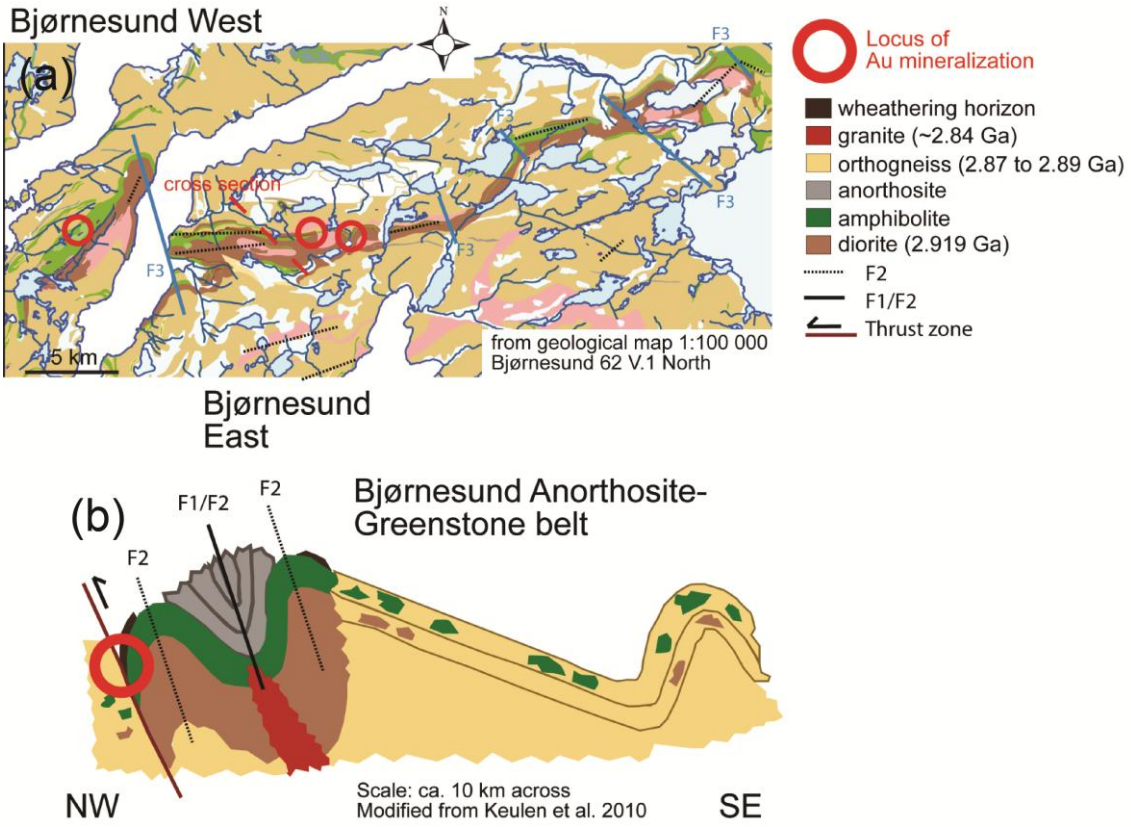

Figure 26. *Relation between the geology and the structural setting and the locus of gold mineralization in the Bjørnesund Greenstone belt.* ***A.*** *Surface map.* ***B.*** *Simplified geological cross section, for location of cross section see Figure 26A. Modified from Keulen et al. (2010a).*

The locus of gold in Bjørnesund East and West is near the meta-qtz-diorite / gneiss contact within shear zones; this zone comprises amphibolite and is at least 10 km long and represents a portion of the entire ~50 km long greenstone belt (Fig: 26A).

Gold mineralization at Bjørnesund East is located in a thin shear zone on the frontal ramp related to F2 folding (compression) and in Bjørnesund West the mineralization is located on the lateral ramp of the F2 thrust-fold (extension) which seems to be more favourable for the introduction of gold (Fig. 26A and B).

The spatial association of gold mineralisations and granite-trondhjemite rocks is intriguing (Fig. 26B).

Although the work carried out under this report was focussed on evaluating the potential for orogenic gold deposits, it should be kept in mind that the Bjørnesund area also contains characteristics typical of areas hosting Ni, Cr, and PGE mineralisations.

An overall compilation of all available geochemical data will allow for more advanced interpretations of gold and orthomagmatic deposits. Good chemostratograpy and mass change calculations will help to better understand the mineralising events. These compilations will lead to a better understanding and a better characterisation of the mineralising event that is associated with the gold mineralisation in the Bjørnesund area. It is also recommended to combine the new data set that stems from this work with the data that were earlier reported by NunaOil A/S in the reports by Heilmann in 1998 and 1997.

It is recommended to map and to systematically sample in detail the newly discovered mineralised shear zone in Bjørnesund West with the purpose of determining gold content and dimension. Such assessment can be done by systematic saw-profiles or chip sampling across the mineralized shear-zone. If there are several mineralized shear-zones present, they should all be systematically described and sampled. Furthermore, it is recommended to test for other gold zones in the Bjørnesund West area and elsewhere in the Bjørnesund greenstone belt.

GEUS is currently carrying out additional work on some of the samples with Scanning Electron Microscope (SEM) in order to characterise hydrothermal alteration and ore minerals. Furthermore, microtectonic studies of the mineralised shear zone are underway. These data will be important to characterize this new gold occurrence in Bjørnesund West.

Acknowledgements

Yong Chen, who stayed as a visiting scientist at GEUS in 2009 (presently at the Shanghai Institute of Geological Survey) is thanked for having participated in the field work. Yong Chen also did the interpretation of ASTER remote sensing data during 2009, just before the field work. His work has helped to better focus the field work, and to carry out field work more efficiently.

Interesting discussions with Jochen Kolb have greatly inspired this work; Jochen is particularity thanked for his ideas about the overall structural interpretation of the Bjørnesund area. Nynke Keulen is thanked for having provided interesting ideas regarding the geotectonic setting of the Bjørnesund area, her interpretations have greatly helped to better present the data in this work. The base camp staff is greatly thanked for having provided all the services from the Midgaard base and for having arranged for pick-up from and to Fiskenæsset, and for having arranged for the handling of samples from Greenland to Copenhagen.

Finally, reviewer Barry L. Reno, GEUS, is thanked for having critically reviewed an earlier version of this report and for having suggested changes which have greatly improved the earlier draft manuscript.

References

Appel, P.W.U. 1992a: Bjørnesund Project, West Greenland. Rapport Grønlands Geologiske Undersøgelse **155**, 24–27.

Appel, P.W.U. 1992b: Tourmalinites in supracrustal rocks in the Bjørnesund area, West Greenland. Rapport Grønlands Geologiske Undersøgelse **155**, 73–78.

Barker, F. 1979: Trondhjemite: Definition, environment, and hypotheses of origin. In: Barker, F., ed., Trondhjemites, Dacites, and Related Rocks, Elsevier, Amsterdam, 1–12.

Barrett, T.J. & MacLean, W.H. 1994: Chemostratigraphy and hydrothermal alteration in exploration for VHMS deposits in greenstones and younger volcanic rocks. In: Lentz DR (ed) Alteration and alteration processes associated with ore-forming systems. Short Course Notes, Volume **11**. Geological Association of Canada, 433–467.

Eilu, P. & Groves, D.I. 2001: Primary alteration and geochemical dispersion haloes of Archaean orogenic gold deposits in the Yilgarn Craton: the pre-weathering scenario. Geochemistry: Exploration, Environment, Analysis **1**: 183-200.

Erfurt, P., Steenfelt, A. & Dam, E. 1991: Reconnaissance geochemical mapping of southern West Greenland from 62°30′N to 64°00′N – 1991 results, Geological Survey of Greenland Open File Series, **91/9**.

Escher, J.C. & Pulvertaft, T.C.R. 1995: Geological map of Greenland, 1:2 5000 000. Copenhagen: Geological Survey of Greenland.

Field Instructions and Standards 2009, edited by Vestergaard M. Geological Survey of Denmark and Greenland, Ministry of Climate and Energy 2010, 142 pages, printed and also available as a pdf file from GEUS.

Groves, D.I., Goldfarb, R.J., Frei, R. & Hart, C.J.R. 2003: Gold Deposits in Metamorphic Belts: Overview of Current Understanding, Outstanding Problems, Future Research, and Exploration Significance. Economic Geology **98**: 1–29.

Heilmann, A., 1998: Exploration within the Bjørnesund linear Belt and Diamond Exploration within the Licence, Licence 14/96, NunaOil A/S, 15 pp., 5 appendices, Open file number 21560.

Heilmann, A., 1997: Mineral Exploration in the Bjørnesund Concession, southern West Greenland, July – September 1996, NunaOil A/S, 18 pp., 6 appendices, Open file number 21515.

Jensen, L.S. & Pyke, D.R. 1982: Komatiites in the Ontario portion of the Abitibi belt In: Komatiites. Geol. (eds) N.T. Arndt & E.G. Nesbitt (Allen and Unwin, London): 147–157

Keulen, N., Schumacher, J.C., van Hinsberg, V., Szilas, K., Windley, B. & Kokfelt, T.F. 2010a: The Bjørnesund anorthosite-greenstone belt - linking the Fiskenæsset complex to the Ravns Storø metavolcanic belt. In: Kolb, J. & Kokfelt, T. F. (eds.). Annual workshop on the geology of southern West Greenland related to field work: abstract volume 2, Danmarks og Grønlands Geologiske Undersøgelser Rapport 2010/58, 9–13.

Keulen, N., Kokfelt, T.F. & Scherstén, A. 2010b: Notes on the common legend to the 1:100 000 digital geological map of southern West and South-West Greenland, 61°30' - 64°N. Danmarks og Grønlands Geologiske Undersøgelse Rapport 2010/119, 40.

Keulen, N., Schumacher J.C., van Hinsberg, V., Szilas, K., Windley, B., Kokfelt, T.F., Schlatter, D.M. & Scherstén, A. 2011: The Bjørnesund anorthosite-greenstone belt - a link between the Fiskenæsset complex and the Ravns Storø metavolcanic belt, southern West Greenland. In: Geophysical Research Abstracts Vol. 13. EGU General As-

sembly 2011; EGU2011-8525-1, 1 p. on flash memory card and downloadable from EGU webpage

Kokfelt, T.F., Keulen, N., Næraa, T., Nilsson, M., Scherstén, A., Szilas, K. & Heijboer, T. 2011: Geochronological characterisation of the felsic rocks of the Archaean craton in South-West Greenland and southern West Greenland, 61°30' – 64°N. Danmarks og Grønlands Geologiske Undersøgelse Rapport **2011/12**, (in press).

Le Bas, M.J., Le Maitre, R.W., Streckeisen, A. & Zanettin, B. 1986: A chemical classification of volcanic rocks based on the total alkali-silica diagram. Journal of Petrology **27**: 745–750.

MacLean, W.H. & Barrett, T.J. 1993: Lithogeochemical techniques using immobile elements. Journal of Geochemical Exploration **48**: 109–133.

McGregor, V.R. & Friend, C.R.L. 1992: Late Archean prograde amphibolite- to granulite-facies relations in the Fiskenæsset region, southern West Greenland. J. Geol. **100**: 207–219.

Minex, Greenland Mineral exploration newsletter no. 35 December 2009, published by BMP and GEUS. K. Secher (ed), 2–3.

McPhie, J., Doyle, M. & Allen, R. 1993: Volcanic textures. A guide to the interpretation of textures in volcanic rocks. Hobart, University of Tasmania, Centre for Ore Deposit and Exploration Studies, 196 p.

Stensgaard, B.M. 2011: En økonomisk geologisk undersøgelse af området mellem Ameralik fjord og Sermiligaarsuk fjord, Sydvestgrønland. En orientering om de opnåede resultater fra en 3-årig indats. In: P. Kalvig & L. Thorning (eds.) 2011, Danmarks og Grønlands Geologiske Undersøgelse Rapport **2011/23**, 18–23.

Stensgaard, B.M. 2008: Gold favourability in the Nuuk region, southern West Greenland: results from fieldwork follow-up on multivariate statistical analysis. Mineral resource assessment of the Archaean Craton (66° to 63°30´N), SW Greenland. Contribution no. 9.Danmarks og Grønlands Geologiske Undersøgelse Rapport **2008/08**, 74 pp.

Myers, J.S. 1985: Stratigraphy and structure of the Fiskenæsset complex, southern West Greenland. Grønlands Geologiske Undersøgelse, Bulletin **150**, 72 pp.

NunaMinerals 2006: Annual Report 2006, dated 30 Apr 2007.

Pearce, J.A. 1996: A user's guide to basalt discrimination diagrams. In: D.A. Wyman (ed) Trace element geochemistry of volcanic rocks: applications for massive sulphide exploration. Geological Association of Canada. Short Course Notes, Vol. **12**: 79–113.

Plimer, I.R. 1988: Tourmalinites associated with Australian Proterozoic submarine exhalative ores. In: G.H. Friedrich & P.M. Herzig (eds.). Base metal sulfide deposits in sedimentary and volcanic environments. Springer, Berlin Heidelberg New York, 255–283.

Pulvertaft, T.C.R. :1972: Preliminary report on the geology of the area between Kigutilik and Bjørnseund (62 V 1). Field diary/report in GEUS archive.

Schlatter, D.M. 2007: Volcanic Stratigraphy and Hydrothermal Alteration of the Petiknäs South Zn-Pb-Cu-Au-Ag Volcanic-hosted Massive Sulfide Deposit, Sweden, Ph.D. thesis, Department of Chemical Engineering and Geosciences, Division of Ore Geology and Applied Geophysics. Luleå University of Technology, ISSN: 1402-1544, 193 pp.

Schlatter, D.M. & Kolb, J. 2011: Host rock composition and hydrothermal alteration as tools for exploration in the Nanortalik gold district In: Conference proceedings, Let's talk ore deposits. 11th Biennial SGA Meeting, Antofagasta, Chile. 3 pp.

Schlatter, D.M. & Christensen, R. 2010: Geological, petrographical and geochemical investigations on the Qussuk gold mineralization, southern West Greenland. In: Nakrem

HA, Harstad AO, Haukdal G (eds) 29th Nordic Geological Winter Meeting, Geological Society of Norway, p. 173.

Schlatter, D.M., Buller, G., Larsen, U. & Stensgaard B.M. 2010: Digital field data capture: the Geological Survey of Denmark and Greenland experiences in Greenland. Explore No. **147**: 2–14

Stenfeldt, A. 2012 (submitted): Analysis of regional datasets for mineral potential considerations based on geological experience. In: B.M. Stensgaard (ed.) Mineral potential mapping for gold in entire southern West Greenland by experience, neural network and self-organising map methods: Danmarks og Grønlands Geologiske Undersøgelse Rapport. 2012/XXX, XXX–XXX.

Stensgaard, B.M. 2008: Gold favourability in the Nuuk region, southern West Greenland: results from fieldwork follow-up on multivariate statistical analysis. Mineral resource assessment of the Archaean Craton (66° to 63°30'N) SSW Greenalnd Contribution no. 9. Danmarks og Grønlands Geologiske Undersøgelse Rapport 2008/8, 74.

Stensgaard, B.M., Rasmussen, T.M. & Steenfelt, A. 2006a: An integrative and quantitative assessment of the gold potential in the Nuuk region, West Greenland. . Geology of Denmark and Greenland Bulletin. Review of Survey Activities 2005. 10, 37-40.

Stensgaard, B.M., Steenfelt, A. & Rasmussen, T.M. 2006b: Gold potential of the Nuuk region based on multi-parameter spatial modelling. Progress 2005. Danmarks og Grønlands Geologiske Undersøgelse Rapport 2006/27, 207.

Stensgaard, B.M. 2012a (submitted) (ed.): Mineral potential mapping for gold in entire southern West Greenland by experience, neural network and self-organising map methods: Danmarks og Grønlands Geologiske Undersøgelse Rapport. **2012/XXX**, XXX pp.

Stensgaard, B.M. 2012b: Analysis of regional datasets based for predictive gold targeting using mathematical neural network analysis. In: B.M. Stensgaard (ed.) Mineral potential mapping for gold in entire southern West Greenland by experience, neural network and self-organising map methods: Danmarks og Grønlands Geologiske Undersøgelse Rapport. **2012/XXX**, XXX–XXX.

Sun, S. & McDonough, W.F. 1989: Chemical and isotopic systematics of oceanic basalts: implication for mantle composition and processes. In: Saunders AD, Norry MJ (eds.) Magmatism in the Ocean basins. Geol. Soc. London, Spec. Publ. **42**: 313–345

Szilas, K., Berger, A., Kokfelt, T.F., Næraa, T., Scherstén, A. & Klausen, M. 2011: Geochemistry of the supracrustal rocks and the associated intrusive TTG suites of the Archaean craton in South-West Greenland and southern West Greenland, 61º30' – 64ºN. Edited by Kokfelt TF. Danmarks og Grønlands Geologiske Undersøgelse Rapport **2011/10**, 88 pp.

Winchester, J.A. & Floyd, P.A. 1977: Geochemical discrimination of different magma series and their differentiation products using immobile elements. Chemical Geology **20**: 325–343.

Windley, B.F., Herd, R.K. & Bowden, A.A. 1973: The Fiskenæsset complex, West Greenland. Grønlands Geologiske Undersøgelse, Bulletin **106**, 80 pp.

List of Appendices on CD-ROM

Appendix A

Electronic field book: GanFeld data from the digital field data capture system (GSC and additional improvements done by GEUS, for details see Schlatter *et al.* 2010). The GanFeld data comprises detailed information of 135 stations. **Appendix A-1** contains the raw data and **Appendix A-2** summarises the captured information for each station.

Appendix B

Photographs from the field work.
Pics DMS, (Pictures from Denis Schlatter); (IMG_0485.jpg to IMG_ 0751.jpg): Each photo has an unique ID number; this ID number relates to a locality and geological information which can be found in Appendix A.

Pics CYO, (Pictures from Yong Chen) ; (IMG_1645.jpg to IMG_0751.jpg): Each photo has an unique ID number; this ID number relates to a locality of DMS. The key linking unique ID number of picture to the GanFeld locality of DMS is given in a table.

Appendix C

Geochemical results as reported by the Actlabs and ACME laboratories (Work orders A09-5687, A09-7612, VAN09005154, VAN09005766).

Appendix D

Geochemical data combined with the most important field data from GanFeld.

Appendix E

Protocol of sample preparation applied to 56 Bjørnesund stream and scree sediment samples.

Appendix F

Chemical classification of all 73 rock-samples of this study. Each sample is classified in one of the 19 chemical rock classes. Trondhjemite, TTG gneiss, basalt A, basalt B, basalt C, basalt D, basalt E, basalt F, basalt Ti, basalt X, amphibolite-gneiss, Qtz-dioritic gneiss, Qtz-

plagioclase-hbl rock, Anorthosite, Dolerite dyke, Gabbro, High Mg-Cr-Ni-Co basalt, High Ti-Zr basalt and Ni-rich basalt.

Appendix G

Graphical log of the surface profile in Bjørnesund East (for details of the method of graphical logging see McPhie *et al.* 1993).

Copy of field notes taken by Denis Schlatter during the field work in the Bjørnesund area. (Geological information taken in addition to the information in Appendix A).

Appendix H

Relevant geo-information of samples that were sent to the Lund University for geochronological studies.

Appendix I

Two PowerPoint presentations by Denis Schlatter & Bo Møller Stensgaard summarising project progress. These presentations were given to the BMP in order to provide information about the progress of the on-going work, and the preliminary results.

Appendix J

EPMA data and BSE pictures from probe work done by a JEOL JXA-8200 superprobe at the Geological Institute in Copenhagen; microphotographs of probed spots.